Title: Alcohol Dependence differentially alters Orbitofrontal Cortex Representations of Inferred Decision-Making and Outcomes

Authors and author addresses:

Christian Cazares[1], Drew C. Schreiner[2], and Christina M. Gremel[1,2].

[1]The Neurosciences Graduate Program, University of California San Diego, La Jolla, CA 92093, USA

[2]Department of Psychology, University of California San Diego, La Jolla, CA 92093, USA

Correspondence:

Christina M. Gremel, Ph.D.

University of California San Diego

9500 Gilman Drive, Mail Code 0109

La Jolla, CA 92093-0109

858-594-8933

E-mail: cgremel@ucsd.edu

Abstract

Alcohol dependence results in neurocognitive disorders, including long-lasting deficits in decision-making processes. Neurobiological investigations have identified the orbitofrontal cortex (OFC) as a key node in inference and outcome-based decision-making, and alcohol dependence alters OFC function. However, which contributing neural computations are disrupted in alcohol dependence is unclear. Here, we combined a well-validated mouse model of alcohol dependence with in vivo extracellular recordings during decision-making. Using an action differentiation task where lever press duration is inferred from an internal associative map and made with regard to outcome value, we identified disruptions to OFC-based computations. Interestingly, alcohol dependence increased OFC activity representing inference-based lever-pressing, but decreased OFC activity during outcome devaluation. This suggests alcohol dependence induces a long-lasting disruption to OFC representations of decision-making such that action representation in enhanced, but OFC contributions to evaluating consequences is diminished. This has important implications for hypotheses regarding compulsive and habitual phenotypes observed in addiction.

Key words: Alcohol, Devaluation, Orbitofrontal Cortex, Compulsive, Dependence, Action

Introduction

Alcohol use disorder results in neurocognitive dysfunction (DSM-5, 2013). For instance, alcoholic patient studies consistently report long-lasting decision-making deficits that are thought to contribute to habitual and compulsive alcohol-seeking, a persistent vulnerability to relapse, and decrements in daily cognitive function (Stephens & Duka, 2008; Berre et al., 2012; Reich & Goldman, 2015; Le Berre et al., 2017; Sebold et al., 2017; Bickel et al., 2018). With reports of dependence-induced functional and structural alterations across the cortex (Volkow et al., 1994, 1997; Laakso et al., 2002; Cardenas et al., 2011; Durazzo et al., 2011; Beck et al., 2012; Sjoerds et al., 2013; Thayer et al., 2016), it is highly likely that a broad array of computations normally contributing to efficacious decision-making are also altered. Identifying which computations are disrupted along with any corresponding aberrant activity patterns would offer a starting point for mechanistic investigations into cortical circuit alterations that produce impaired decision-making.

One such area that often shows dependence-induced disruptions is the orbital frontal cortex (OFC). Alcoholic patient studies generally report a hypoactive OFC both at baseline and during adaptive decision-making (Volkow et al., 1994, 1997; Boettiger et al., 2007; Sjoerds et al., 2013; Reiter et al., 2016), but also report OFC hyperactivity to stimuli and related approach behaviors (Wrase et al., 2002; Tapert et al., 2003; Myrick et al., 2004; Hermann et al., 2006; Myrick et al., 2008; Ernst et al., 2014; Reinhard et al., 2015), reminiscent of OFC hyperactivity reported in patients with other psychiatric conditions, including obsessive compulsive disorder (Milad & Rauch, 2012; Pauls et al., 2014; Robbins et al., 2019; Lüscher et al., 2020). This dichotomy of effects suggests that perturbations to OFC circuitry induced by alcohol dependence may subsequently alter the computations performed by OFC neurons in response to information coming into OFC. Hence, initial investigations into computations performed by OFC during decision-making and their disruption in alcohol dependence would provide a framework with which to investigate broader circuit mechanisms contributing to observed OFC dysfunction.

Several lines of evidence implicate the OFC as a key regulator of the neurobiological circuitry supporting decision-making processes (Fellows, 2007; Wallis, 2007; Gremel & Costa, 2013; Stalnaker et al., 2015; Padoa-

Schioppa & Conen, 2017). In particular, recent works have supported the hypothesis that the OFC may serve as a cognitive map, supporting inference of unobservable learned information necessary to guide flexible behavior (Wilson et al., 2014; Baltz et al., 2018; Schuck et al., 2016; Niv, 2019; Malvaez et al., 2019; Zhou et al., 2019). Indeed, OFC has long been known to convey unobservable information about changes in outcome values and their contingent choices or actions to guide decision-making. Animal models of alcohol dependence have revealed long-lasting dependence-induced disruptions to OFC dependent processes including behavioral flexibility and outcome devaluation (Badanich et al., 2011; Kroener et al., 2012; M. F. Lopez et al., 2014; Fernandez et al., 2017; Renteria et al., 2018, 2020). Ethanol dependence results in long-lasting changes to OFC intrinsic excitability and synaptic transmission, as well as increases in dendritic spine density of OFC neurons (Badanich et al., 2013; McGuier et al., 2015; Nimitvilai et al., 2016; Nimitvilai, Lopez, et al., 2017; Nimitvilai, Uys, et al., 2017; Renteria et al., 2018). We previously reported that alcohol dependence reduced OFC excitability and produced a loss of goal-directed control assessed via outcome devaluation using sensory-specific satiety. Notably, artificially increasing the activity of OFC projection neurons was sufficient to restore sensitivity to outcome devaluation in alcohol dependent mice (Renteria et al., 2018). To this end, dependence-induced deficits in decision-making flexibility are hypothesized to include a breakdown of OFC computations critical for inferred representations, especially when direct information about ongoing processes and future consequences is not readily available (Wilson et al., 2014). However, it remains unclear how computations supporting decision-making are represented by OFC neurons and which computations, if any, are disrupted following the induction of alcohol dependence.

Here, we examined dependence-induced disruptions to OFC computations performed during inferred decision-making. To do so, we adapted the instrumental task of action differentiation (Platt et al., 1973; Kuch, 1974; Yin, 2009; Fan et al., 2012), where a mouse must learn to press and hold a lever down beyond a minimum duration to produce a reward. Importantly, this task requires that an animal form an internal associative map to infer the arbitrary minimum duration and thus select the appropriate action plan that will produce a reward. Daily performance was largely intact in alcohol dependent mice, allowing for future comparisons of associated neural activity in the absence of any gross behavioral performance differences. However, follow-up devaluation

testing recapitulated the reduced sensitivity to outcome devaluation previously observed, suggesting dependence-induced alterations to behavioral control over decision-making. The structure of behavior within the task allowed us to assess whether OFC activity reflected computations related to inference and outcome evaluation and whether alcohol dependence affected these dynamics.

Results

Induction of ethanol dependence disrupts goal-directed control over decision-making

We employed a well-validated model of chronic intermittent ethanol vapor exposure and repeated withdrawal (CIE) previously shown to disrupt OFC-based decision-making (H. C. Becker & Hale, 1993; Howard C. Becker & Lopez, 2004; Marcelo F. Lopez & Becker, 2005; Griffin et al., 2009). Mice were exposed to periods of ethanol (CIE) or air (Air) vapor and subsequent withdrawal over a period of four weeks (one vapor cohort; Air: n = 8, CIE: n =7) (Figure 1A). CIE procedures produced mean blood ethanol concentrations in ethanol-exposed mice in line with previous reports (29.53 ± 2.36 mM) (Marcelo F. Lopez & Becker, 2005; Renteria et al., 2018). 72 hours after the last week of vapor exposure, mice were food restricted to achieve 85-90% of their baseline weight for 2 days prior to instrumental training and testing procedures.

To examine the effects of CIE on OFC activity correlates of decision-making, we used a task that engages OFC processes and produces levels of behavior conducive to discretized neural activity analyses of decision-making. Specifically, we adapted an instrumental task examining the temporal differentiation of actions, such that animals had to infer an arbitrary duration criterion from previously experienced action-outcome contingencies (Yin, 2009; Fan et al., 2012). Mice learned to press and hold down a lever for at least a pre-determined minimum duration in order to earn a food pellet upon release of the lever. Throughout individual sessions, mice would self-initiate and self-terminate every lever press in the absence of any extrinsic cues signaling lever press duration. Importantly, reward delivery occurred only at the offset of a lever press that exceeded the duration criteria (Figure 1B), preventing the use of reward presence to signal lever press termination.

Following vapor procedures, and after initial lever press training (see Materials and Methods), Air and CIE mice underwent action differentiation training, with the initial criterion for lever press duration set at 800-ms for 5 days, followed by 5 days of a 1600-ms criterion (see Materials and Methods) (Figure 1A). Across the 800-ms criteria training days, all mice showed similar levels of overall lever press responses, but we did observe initial differences between groups in the percent exceeding the duration criterion (two-way repeated measures ANOVA (Session x Treatment); interaction: $F(4, 52) = 3.13$, $p=0.02$; main effect of Session: $F(4, 52) = 12.62$, $p<0.0001$), as well as lever-pressing rate (two-way repeated measures ANOVA (Session x Treatment); no interaction, main effect of Session: $F(4, 52) = 3.69$, $p=0.01$; main effect of Treatment: $F(1, 13) = 4.90$, $p=0.04$) (Figure 1 — figure supplement 1A-C). A post-hoc comparison of the percentage of lever presses that exceeded the duration criterion found a difference between treatment groups in day 5 of the 800-ms duration criterion sessions ($p=0.02$). However, as training progressed to the 1600-ms criterion sessions, these differences disappeared, such that mice showed similar evidence of learning. For example, there was similar acquisition performance with respects to the average total number of lever presses made between groups (two-way repeated measures ANOVA (Session x Treatment); no interaction; main effect of Session: $F(4, 52) = 9.770$, $p<0.0001$), as well as similar average percentage of lever presses made that exceeded the duration criterion within a session (two-way repeated measures ANOVA (Session x Treatment); no interaction; main effect of Session: $F(4, 52) = 8.723$, $p<0.0001$) (Figures 1D and 1E). In addition, we found comparable learning-related shifts in the distribution of lever-press durations across acquisition of the two duration criteria in both Air and CIE mice (Figure 1 — figure supplement 1D and 1E). We did observe lever-pressing rate differences, with Air mice showing a higher response rate across the five days of 1600-ms criterion than did CIE mice (two-way repeated measures ANOVA (Session x Treatment); interaction: $F(4, 52) = 4.80$, $p=0.002$; main effect of Session $F(4, 52) = 17.34$, $p<0.0001$; Treatment: $F(1, 13) = 5.83$, $p=0.03$) (Figure 1F).

Because we observed learning related shifts in duration distributions, we also directly compared the distributions of all lever press durations in well-trained Air and CIE mice (occurring throughout days 4 and 5 of the 1600-ms duration criteria sessions) and found CIE mice had longer lever press durations compared to Air controls (unpaired t test with Welch's correction, $t_{3533}=6.31$, $p <0.0001$) (Figure 1G). To examine whether this

difference in duration distribution produced different reward rates across a session, we compared the proportion of lever presses that exceeded the 1600-ms duration criterion within equidistant duration bins throughout each individual session. We found similar levels of rewarded lever presses between Air and CIE mice (Mixed-effects model with Geisser-Greenhouse correction, $p>.09$) (Figure 1H). Our results thus far indicate that CIE mice and Air controls can readily acquire similar levels of lever pressing and action differentiation performance for food. However, the difference in response rates and the rightward shift in the duration distribution observed suggests that CIE mice may be doing so under different behavioral controllers.

To directly assess whether outcome value was controlling decision-making, we used an outcome devaluation procedure. Prior work using other types of reinforcement schedules have found that alcohol dependence disrupts the OFC-dependent ability to update and infer a value representation to guide decision-making (Dickinson, 1985; M. F. Lopez et al., 2014; Renteria et al., 2018). We performed outcome devaluation testing following the five days of action differentiation on the 1600-ms duration criterion, and within a time period (21 days following the last vapor exposure) when disruption of outcome value control has previously been observed (Renteria et al., 2018). We subjected Air and CIE mice to sensory-specific satiation of food pellets previously earned by lever pressing or to a previously habituated control outcome (20% sucrose solution). In each of the two consecutive test days, mice had ad-libitum access to either pellets (devalued state) or sucrose solution (valued state) for 1 hour. Following this pre-feeding period, we measured non-reinforced lever press responses during 10-minute sessions of the action differentiation task under a 1600-ms criterion. A reduction in lever-press responses in the devalued state compared to valued state, reflects a sensitivity to outcome value change (Dickinson, 1985). We performed a two-way repeated measures ANOVA (State x Treatment) to examine whether treatment groups showed different patterns of responding. There was no interaction, but there were main effects of State ($F(1, 12) = 10.45$, $p=0.01$) and Treatment ($F(1, 12) = 7.133$, $p=0.02$). This suggests there was a difference in the level of lever pressing between groups during testing and that overall responding was greater on valued than devalued days. To test our a priori hypothesis that CIE procedures would reduce the sensitivity to outcome devaluation procedures (i.e. reduced magnitude effect), pre-planned post-hoc comparisons showed a significant difference between devalued and valued lever pressing only in Air

animals (p=0.01), but not CIE mice (Figure 1I). In contrast, the proportion of successful lever presses that exceeded hold down criteria remained similar across states for both treatment groups (p>0.3) (Figure 1J).

Thus, while CIE exposed mice largely performed the task at similar levels to Air mice, devaluation testing revealed that CIE exposed mice were less sensitive to outcome devaluation. As control and CIE mice consumed similar amounts during the devalued state pre-feeding period (unpaired t test with Welch's correction, $t_{10.7}$=1.864, p > 0.05), differences in palatability or satiety are not likely to contribute to the lack of goal-directed control in CIE mice (Figure 1 — figure supplement 1G). Rather, prior CIE exposure reduced the ability to update and infer outcome value information necessary to guide adaptive decision-making. That this was observed 3 weeks after the last exposure to ethanol vapor lends support to previous findings that alcohol dependence induces a long-lasting breakdown in decision-making processes.

OFC populations differentially encode decision-making performance

Given that the deficits in outcome devaluation observed in CIE mice have been shown to involve the OFC (Gourley et al., 2013; Gremel & Costa, 2013; Rhodes & Murray, 2013; Gremel et al., 2016; Renteria et al., 2018), we hypothesized that alcohol dependence would disrupt OFC neural activity during decision-making. We implanted additional cohorts of mice with chronic indwelling micro-electrode arrays into the OFC prior to the start of vapor procedures and action differentiation lever press training (five vapor cohorts; Air n = 9, CIE n = 9) (Figure 2 — figure supplement 2A and 2B). The similarity of daily performance between Air and CIE mice allowed us to compare associated neural activity in the absence of any gross behavioral performance differences (Figure 2 — figure supplement 1).

We focused on neural activity data collected during the last two sessions that had a 1600-ms duration criterion, a time-point during which animals proficiently performed the task. Putative single OFC unit spike activity was collected during these two sessions and aligned to timestamps collected each time a lever press onset, offset, or pellet reward delivery occurred (see Materials and Methods). Peri-event heatmaps of normalized firing activity suggested a bi-directionality of OFC unit activity modulation present in both Air and CIE animals

(Figures 2A and B). This was observed with respect to lever press onset and offset, suggesting a varied role of OFC neurons in the representation of decision-making initiation and termination. We then identified statistically significant firing in these units with respect to changes from a pre-lever press onset baseline period (see Materials and Methods). We found that OFC units significantly modulated their firing activity across multiple task components (e.g. both the onset and offset of a lever press), as well as in a discrete manner (e.g. only the onset of a lever press) (Figure 2 — figure supplement 2E). Baseline firing rates, modulation unit proportions, and events encoded were similar between Air and CIE animals ($p>0.05$) (Figure 2C, Figure 2 — figure supplement 2C-G).

To examine how OFC activity correlates of decision-making varied with respect to task performance, we first segmented lever press durations by whether they successfully exceeded the lever press duration criterion or not. Individual raster plots of significantly modulated units suggested a predictive quality and rigidity to this encoding. For example, the representative unit shown significantly modulated its firing around the onset and offset of a lever press (Figure 2D and 2E). Most notably, the magnitude of this modulation appeared to be related to the future outcome of the lever press itself. For instance, the same unit that significantly modulated its firing around the offset of a lever press showed a greater change in firing rate when it was a lever press that successfully exceeded the duration criterion (Figures 2F and 2G).

The outcome sensitivity of OFC firing magnitudes was considerably pronounced in both Air and CIE mice such that a support vector machine model trained with the peri-event activity of all captured units could accurately classify whether an individual lever press succeeded in exceeding the 1600-ms duration criterion, reaching peak performance soon after the offset of a lever press in both groups (Figures 2H and 2I). Two-way repeated measures ANOVA (Bin x Treatment) comparisons of temporally binned classification performance between Air and CIE mice revealed no significant differences within the 1 second period prior to lever press onset ($p>0.29$), whereas the classifier showed significantly higher performance accuracy in Air than CIE mice 1 second after the offset of the lever press (interaction: ($F(9, 180) = 3.33$, $p=0.0009$; main effect of Bin only: $F(9, 180) = 5.11$, $p<0.0001$) (Figures 2H and 2I, Figure 2 — figure supplement 2H and 2I). In line with these findings, when we

examined the average z-scored firing rate changes of significantly modulated units based on whether lever presses were successful or not, we saw no differences prior to action onset that were predictive of future performance. However, we did see that shortly after the lever press offset, OFC activity reflected whether that lever press was successful or not for both groups (Figure 3 — figure supplement 1). The relative lower decoder performance in CIE mice at the decision offset, when outcome may or may not have been delivered, suggests reduced contributions of OFC activity to outcome evaluation, a hallmark of OFC function (Stalnaker et al., 2015; Wallis, 2007). Our results thus far support a multifunctional role for the OFC, such that the initiation and cessation of decision-making actions, as well as their associated consequences, are generally represented in the OFC. Furthermore, this representation is altered following alcohol dependence.

Prior chronic alcohol exposure alters encoding of inferred decision-making initiation and outcome evaluation. Given the differentiation of performance outcome by OFC neurons in both Air and (albeit to a lesser degree) CIE mice, we asked whether OFC activity would similarly reflect inferred decision-making between groups, and whether any observed differences would be limited to potential periods of outcome evaluation. To this end, we compared averaged z-scored activity around periods of inferred decision-making, namely before the lever press onset and after the lever press offset, as well as during the evaluation period immediately following reward delivery. We did this for OFC neurons that significantly increased or decreased firing rates from a pre-lever press onset baseline period (see Materials and Methods).

CIE mice showed differences from Air mice in OFC activity across all decision-making epochs. First, when we examined OFC units that significantly increased their firing rates, those belonging to CIE mice showed greater up-modulation prior to lever-press onset, as well as following the offset of a lever press (Figures 3A and 3B) than those belonging to Air mice. Likewise, CIE mice showed less down-modulation of unit activity prior to lever press onset (Figure 3C, left).

A two-way repeated measures ANOVA (Bin x Treatment) of up-modulated unit activity prior to lever press onset showed no interaction, but main effects of Bin ($F(3, 564) = 12.34$, $p<0.0001$) and Treatment ($F(1, 564) =$

5.88, p=0.02) (Figure 3A, left). Similarly, the same analysis performed on activity following the offset of a lever press again revealed no interaction, but similar main effects of Bin ($F(3, 748) = 21.82$, $p<0.0001$) and Treatment ($F(1, 748) = 8.16$, $p=0.004$) (Figure 3A, right). A two-way repeated measures ANOVA (Bin x Treatment) showed treatment differences of down-modulated neural activity prior to lever press onset (no interaction; main effects of Bin: $F(3, 508) = 25.11$, $p<0.0001$) and Treatment: $F(1, 508) = 38.84$, $p<0.0001$) (Figure 3C, left). However, similar analyses on activity following lever press offset and immediately following reward delivery revealed no differences between the down-modulation of OFC activity in Air and CIE animals ($p>0.2$) (Figure 3C, right, and Figure 3D).

In contrast, when we examined increases in OFC activity following reward delivery, we observed the opposite pattern. During this outcome evaluation period, units belonging to Air mice showed greater increases in modulation than CIE mice (Figure 3B). It is important to note here that this unit population differed from OFC units that significantly modulated their firing at lever press offset, as not all units that did so also significantly modulated their firing at outcome delivery. This meant that there were units that selectively responded only to outcome delivery. A two-way repeated measures ANOVA (Bin x Treatment) performed on up-modulated units following reward delivery supported this finding, showing an interaction ($F(3, 532) = 4.51$, $p=0.004$), and a main effect of Treatment ($F(3, 532) = 7.2$, $p<0.0001$). A post-hoc comparison on up-modulated unit activity following found a difference between treatment groups in the second 250-ms bin outcome delivery ($p=0.03$). However, OFC units that down-modulated their firing rate did not differ between groups ($p>0.2$) (Figure 3D).

The above analysis on action initiation and cessation included both rewarded and non-rewarded presses. As both Air and CIE groups could similarly perform the task, we next reasoned that successful decisions would recruit similar levels of OFC modulation. Thus, we examined OFC activity changes occurring only during rewarded action differentiation, specifically when lever presses crossed the arbitrary duration threshold (see Materials and Methods). We found similar levels of OFC activity up-modulation between Air and CIE mice prior to lever press onset and following lever press release (Figure 3 — figure supplement 2A). Two-way repeated measures ANOVA (Bin x Treatment) of significantly up-modulated unit activity found no interactions or effects

of Treatment, but main effects of Bin prior to lever press onset ($F(3, 564) = 6.57$, $p=0.0002$) and offset ($F(3, 748) = 6.04$, $p=0.0005$). However, we also found less down-modulation of OFC activity in CIE mice prior to lever pressing (Figure 3 — figure supplement 2B) (two-way repeated measures ANOVAs (Bin x Treatment): no interaction, main effects of Bin ($F(3, 508) = 14.44$, $p<0.0001$) and Treatment ($F(1, 508) = 28.36$, $p<0.0001$). Furthermore, of OFC units that were initially down-modulated at offset, the subsequent increase in firing rate was larger in Air than CIE mice (two-way repeated measures ANOVA (Bin x Treatment): no interaction, main effects of Bin ($F(3, 328) = 5.02$, $p=0.002$) and Treatment ($F(1, 328) = 9.10$, $p=0.003$).

Our results showed that CIE exposure alters OFC computations made during decision-making. CIE mice showed a modulation of OFC activity that suggests overall increases in OFC activity during actions (i.e. onset and offset), and a blunting of OFC activity during reward evaluation. This suggests that incoming information into the OFC contributing to action inference and outcome evaluation are differentially disrupted following alcohol dependence.

Prior chronic alcohol exposure alters encoding of ongoing decision-making

The nature of the ongoing action differentiation behavior elicited by our task, during which a mouse must hold down the lever, provides an uninterrupted period during which we can measure the underlying OFC neural activity correlates of inferred decision-making. Importantly, the structure of the behavior within the task allowed us to ask 1) whether OFC activity reflected computations arising *during* continuous self-initiated decision-making and 2) whether alcohol dependence affected these dynamics. To do this, we first interrogated spike activity occurring during temporally equivalent duration segments of a lever press between Air and CIE mice (see Materials and Methods). Due to the variable timings of each lever press duration, our analysis focused solely on units that were significantly modulated before the onset of a lever press.

When we examined individual unit activity raster plots, we observed broad reductions in OFC activity, relative to lever press onset, during the execution of action differentiation (i.e. during the lever press itself). Importantly, the magnitude of these reductions appeared to depend on the duration of the lever press (Figure 4A). We first asked whether CIE generally affected this apparent OFC activity reduction. We found that CIE mice trended

toward having a greater proportion of lever presses where OFC up-modulated units continued to fire while holding down the lever (unpaired t test with Welch's correction, $t_{138.4}$=1.899, p=0.06) (Figure 4B), but observed no differences between groups in their respective down-modulated populations (p>0.2) (Figure 4D).

We next wanted to examine whether there was any evolution of OFC activity across the duration of a lever press. We began by dividing each lever press into four equal duration segments and looking at the average proportion of total spikes that occurred within each individual segment. We uncovered a U-shaped distribution of activity across the duration of a lever press in Air mice that was absent in CIE mice (Figure 4C). For example, in Air mice, spikes occurred more often during the initial segment of the lever press, then diminished in the middle portions, prior to once again increasing in occurrence immediately before lever press offset. This U-shaped distribution pattern of spike activity was significantly altered in CIE mice. A two-way repeated measures ANOVA (Segment x Treatment) showed a significant interaction (F(3, 564) = 3.270, p=0.02), and a main effect of Segment (F(3, 564) = 18.64, p<0.0001). Post-hoc comparisons within Air mice found that the proportion of spikes during the beginning and end (first and last lever press segments) differed from the proportion of spikes observed during the middle of a lever press (second and third segments (p<0.05). However, in CIE mice, only the proportion of spikes during the first segment differed from the proportion of spikes during second and the third segments (p<0.05). Furthermore, the noticeable rise of activity at the end of the lever press (i.e. in the last segment) observed in Air mice was absent in CIE mice. Indeed, a between-groups post hoc comparison found a significantly lower proportion of spikes in the last segment prior to lever press release in CIE mice compared to Air mice (p<0.05) (no other segments differed, p>0.29). In contrast, we found no difference between Air and CIE mice in the distribution pattern of ongoing spike activity from down-modulated units, with the proportion of total spikes generally increasing the closer the segment was to the offset of the lever press (two-way repeated measures ANOVA (Segment x Treatment): no interaction or main effect of Treatment, main effect of Segment (F(3, 508) = 39.18, p<0.0001) (Figure 4E).

Considering the observed change in spike distribution across the duration of the lever press, we hypothesized that OFC firing rates during action differentiation may differentially modulate with respect to the prospective

duration of the ongoing, executed lever press. That is, the longer the lever press, the greater modulation of OFC activity. In addition, we hypothesized that ethanol dependence may also alter this activity-duration relationship. To examine this, we first segmented each lever press duration and its underlying spike activity and then grouped them into duration quartiles determined by within-session lever press distributions (see Materials and Methods). For example, all lever presses that an individual mouse made within a single session were equally divided into four segments determined by the total duration of the lever press, and all of the corresponding segmented OFC unit activity tied to the lever press was assigned to one of the four duration quartiles and z-scored correspondingly (Figures 5A and B, Figure 5 — figure supplement 1A). Even with the previously observed, slight rightward shift in the distribution of lever press durations in CIE mice (Figure 1G), the duration bin edges of these quartile distributions were similar between Air and CIE mice (Figure 5 —figure supplement 1B and 1C). Within each quartile distribution, we then binned z-scored firing-rates into 4 equal sized segments across the duration. We did this separately for neurons that were significantly up-modulated or down-modulated at lever press onset. This allowed us to make treatment group comparisons of OFC spiking activity that occurred across action differentiation with regards to the future, total duration of the ongoing action.

These analyses uncovered two notable findings. First, we found that OFC activity showed a dynamic shift in firing rate modulation during the lever press that depended on the future duration. That is, lever presses of different durations had different patterns of OFC activity. Second, prior CIE exposure altered the firing rates occurring during the execution of action differentiation (i.e. during the lever press itself). When we examined OFC neurons that were increasing their activity at lever press onset, we found that average z-scored firing rates during longer lever presses (only in the 3rd and 4th quartiles), reflected the U-shape spike activity previously observed (Figures 5C-F). A two-way repeated measures ANOVA (Segment x Treatment) performed within each duration quartile showed a main effect of Segment for the 3rd quartile ($F(3, 560) = 3.339$, $p=0.02$) and 4th quartile ($F(3, 560) = 7.205$, $p<0.0001$). Interestingly, while there was a main effect of Treatment observed in the 1st quartile ($F(1, 560) = 12.45$, $p=0.0005$), no other main effects of Treatment or interactions were observed. Hence, OFC units in Air and CIE mice that increased their firing rate at lever press onset

showed a similar U-shaped pattern of firing rate modulation that was present only when lever presses were of relatively longer duration. Notably, not all lever press durations within the 3rd and 4th quartiles exceeded the duration criteria, rather only a fraction of these lever presses actually produced a reward. This suggests that differential patterns of OFC activity may emerge prior to the release of a lever press. This modulation pattern of OFC activity with respect to lever press duration may reflect an inferred action-outcome contingency guiding action differentiation.

We found treatment differences between Air and CIE mice in neurons that decreased their activity prior to lever press onset. These OFC neurons did not show a U-shape pattern of firing rate change (Figures 5C-F). Instead, down-modulated OFC units largely showed a gradual return towards baseline rates prior to lever press release, and the magnitude of this down-modulation differed between treatment groups. For most of the duration quartiles (except for the 1st quartile, which contained the shortest lever presses within a session), there was a reduction in the down-modulation (i.e., an increase) of OFC activity across the duration of a lever press. Furthermore, two-way repeated measures ANOVAs (Segment x Treatment) revealed that the observed down-modulation was greater in Air than CIE mice in the 2nd (main effect of Segment: $F(3, 508) = 3.262$, $p=0.02$; main effect of Treatment: $F(1, 508) = 33.75$, $p<0.0001$) and 3rd quartiles (main effect of Segment: $F(3, 508) = 4.923$, $p=0.002$; main effect of Treatment: $F(1, 508) = 4.658$, $p=0.03$). However, in the 4th quartile, this group difference reversed, with the longest and most often rewarded lever presses being accompanied by stronger down-modulation of OFC activity in CIE than Air mice (main effect of Segment: $F(3, 508) = 10.26$, $p<0.0001$; main effect of Treatment: $F(1, 508) = 4.069$, $p=0.04$).

Follow-up comparisons of average z-scored firing rates between quartiles in Air and CIE mice revealed that changes in activity magnitude following the offset of a lever press were by and large reflective of the duration of the just released lever press. For instance, ordinary one-way ANOVAs on up-modulated unit activity showed that lever press durations that were included in the 4th quartile, the longest of all lever presses, had the greatest change in firing in both Air and CIE mice ($p<0.05$) (Figure 5 — figure supplement 2A). A similar analysis performed on down-modulated unit activity showed that this duration-related effect was only present in

Air ($p<0.05$) but not CIE ($p>0.05$) mice (Figure 5 — figure supplement 2B). These findings suggest that 1) OFC activity post-decision is still influenced by the inferred and executed action contingency (independent of outcome delivery), and 2) that this representation may be altered following alcohol dependence.

Discussion

Alcohol dependence is associated with impairments to OFC function thought to contribute to aberrant decision-making, thereby increasing the vulnerability to relapse and maladaptive alcohol consumption (Zinn et al., 2004; Chanraud et al., 2007; Loeber et al., 2009; Berre et al., 2012; Reiter et al., 2016; Le Berre et al., 2017). Here, we uncovered neural correlates of decision-making and found them perturbed by prior chronic alcohol exposure and withdrawal. Our results suggest alcohol dependence induces long-lasting perturbations to OFC activity in a bidirectional manner, dependent on the decision-making computation being performed. Alcohol dependence led to increases in activity prior to action onset and reduced activity during outcome evaluation. This suggests that alcohol dependence does not result in a loss of OFC contributions, but rather induces a change in how information in OFC circuits could be used to control decision-making.

In the present data, CIE exposed animals acquired and performed the action differentiation task at similar levels compared to alcohol naïve controls when the value properties of the pellet outcome remained stable across training, suggesting that the acquisition of associative information was unperturbed in alcohol dependence (Figure 1). However, while Air mice adjusted responding following outcome devaluation, CIE mice did so to a lesser degree. Hence our action differentiation task was shown to effectively isolate instrumental learning contingency processes from those crucial for updating and inferring value representations, with the unique feature of doing so in a completely self-paced manner that requires an animal to continuously infer contingency durations to guide their behavior. The comparable levels of performance in our task, and the differences observed following outcome devaluation, suggests that the effects of alcohol dependence on behavioral control might be somewhat limited to those requiring value change processes. However, how and whether action contingency and outcome value processes influence each other is not clear. Our data does suggest that further exploration into alcohol dependence effects on action contingency control is warranted.

Clinical studies have previously shown how alcohol dependence alters representation of decision-making within OFC circuits, albeit not always in the same manner. The OFC is widely found to be hypoactive in alcohol dependence (Volkow et al., 1994, 1997; Boettiger et al., 2007; Sjoerds et al., 2013; Reiter et al., 2016), but there have also been reports of hyperactivity (Wrase et al., 2002; Tapert et al., 2003; Myrick et al., 2004; Hermann et al., 2006; Myrick et al., 2008; Ernst et al., 2014; Reinhard et al., 2015). We find that to be the case in our data as well, such that alcohol dependence altered decision-making representations in the OFC in a variety of ways. Prior CIE exposure and withdrawal changed OFC computations related to decision-making actions in a way that suggests an overall increase in activity (Figure 3). This dependence-induced change present in both up- and down-modulated unit populations during action initiation, as well as in the up-modulated population following action release, suggests an increased contribution of OFC processes to decision-making actions. We should emphasize that the action contingency in the present task is the duration of the lever press, and that it is inferred from previously learned associations. This suggests that alcohol dependence increases OFC activity related to the retrieval and execution of inferred action contingencies. In this context, it is important to note that a hyperactive OFC has also been observed in those with obsessive compulsive disorder and increased activity of OFC neurons during actions has been linked to compulsive action phenotypes (Milad & Rauch, 2012; Pauls et al., 2014; Robbins et al., 2019; Lüscher et al., 2020).

A hallmark of OFC function is its contribution to outcome evaluation and updating, with increases in OFC activity observed during outcome presentation (Jones et al., 2012; Stalnaker et al., 2014, 2015, 2018). Recent works have shown that inhibition of OFC activity during periods of reward presentation prevent outcome evaluation and updating (Baltz et al., 2018; Malvaez et al., 2019). Here, we observed large increases in OFC activity during outcome evaluation periods and this increase was reduced following alcohol dependence (Figure 3). SVM modeling showed reduced accuracy in classifying rewarded lever presses following the induction of dependence (Figure 2). Furthermore, CIE affected OFC computations made only after successful lever presses, once again selectively altering our up-modulated unit population, except now by blunting activity soon after delivery of the food reward (Figure 3). Thus, in addition to action-associated OFC activity, the data above strongly suggests that OFC's contribution to outcome evaluation is reduced following alcohol dependence. However, in the current experiments we did not test whether the observed increases and

decreases in activity correspond with increased and decreased contributions of OFC to decision-making. Nonetheless, the observed bidirectional dependence-induced effects on OFC computations support the hypothesized complexity of alcohol dependence effects on OFC decision-making circuitry. For instance, previous accounts on the modulatory influence of alcohol dependence on OFC activity have differed (Volkow et al., 1994, 1997; Boettiger et al., 2007; Sjoerds et al., 2013; Reiter et al., 2016), which in conjunction with our findings suggests a divergent effect of alcohol dependence that may be dependent on decision-making demands and corresponding afferent activity into the OFC. While the critical role for the OFC in regulating the ability to adjust behavior when outcome value changes has been largely established, here we present new evidence on the specificity of dependence-induced effects on the computations supporting these processes.

Our findings lend support to previous work and hypotheses putting forth OFC's critical role in representing self-inference in a continuous fashion (Wilson et al., 2014; Schuck et al., 2016; Niv, 2019; Zhou et al., 2019). Previous work has delineated state representations that are not explicitly associated with external factors, such as environmental stimuli (e.g. a cue light indicating the start of a trial), as "hidden" states that must instead be inferred from retrieved information about context or previous stimulus- outcome or action-outcome contingencies (Wilson et al., 2014; Schuck et al., 2016; Niv, 2019). The analogy presented is like that of a "cognitive map", where the OFC can flexibility represent current task states by determining the present "location", and thus the most appropriate decision-making strategy, based on the multitude of integrated information.

The self-paced nature of our task allowed us to investigate the dynamics of OFC computations made during ongoing decision-making that relies solely on internal representations of task demands, rather than a reliance on predictive external sensory information. Here, we show with in vivo electrophysiology data that the OFC is actively engaged during action differentiation. OFC activity changed throughout individual lever press durations, resembling a U-shaped pattern in our captured up-modulated units that suggest a working process for inferring the proximity to achieving a desired goal (Figure 4). Moreover, these continuous patterns of activity at first reflect an overall decrease occurring during these ongoing inferences, that subsequently increase prior to the release of the lever press and prior to when outcomes are expected (Figure 5). Notably, these patterns were present across a variety of lever press durations, including those that did not produce a reward.

Interestingly, prior alcohol dependence had minor effects on these activity patterns. There was a slight reduction to the increase in OFC activity prior to lever press release (Figure 4). However, analyses dividing lever press by duration suggest that this may be driven by a treatment difference for only the shortest lever presses (Figure 5). Indeed, the U-shaped pattern of OFC activity throughout the duration of the lever press observed in Figure 4C was replicated in the 3rd and 4th duration quartiles, with no observed difference between treatment groups, suggesting that this pattern is strongest during the longest lever presses.

We propose that within this framework, the present observed OFC patterns of activity could reflect how the OFC continuously integrates unobservable information for action execution, such as the inferred duration of the lever press and previous subjective history with the session's duration criterion, to determine whether a desired outcome is likely to occur. As the animal learned the task, subjective experience accumulated and was used to form inferences based on previously learned maps of the associative contingency (e.g. exceeding an inferred duration will result in a food reward). It may be that the patterns of activity occurring before a lever press was initiated reflect a preparatory component of these inferences, such as the selection of a motor plan that could aim to optimize future performance. That both groups showed OFC modulation prior to and during a lever press suggests that initial information used to guide decision-making is still represented and may be enhanced in the OFC following alcohol dependence. Another hypothesis is that the increase in activity prior to lever press release corresponds to the greater confidence in reward delivery, something previously shown for OFC activity in cued tasks (Kepecs et al., 2008; Masset et al., 2020). This hypothesized confidence representation within OFC could be driven by reward expectation that may arise through ongoing inference processes.

The dichotomy of CIE effects on the different behavioral components of our task suggests a combination of OFC circuitry changes that could manifest in a variety of ways. In the future, it will be of interest to examine how CIE perturbs OFC function and output that relies on information received by interconnected structures. For example, chronic alcohol exposure and withdrawal may be perturbing the excitability and transmission of local OFC circuitry via cell-type specific changes (Badanich et al., 2013; McGuier et al., 2015; Nimitvilai, Uys, et al., 2017; Renteria et al., 2018), such that the integration of incoming information from other associative regions necessary to guide decision-making is disrupted. Additional difficulties in parsing the effects of alcohol dependence on decision-making processes arise from a fundamental lack of structural and functional input-

output mapping of the highly complex neural circuits that support decision-making. While in general the areas projecting to OFC have been identified, the relative proportions of inputs across brain regions, as well as the connectivity, strength and pattern of inputs onto excitatory and inhibitory OFC populations is unknown in naïve circumstances, much less following alcohol dependence. It may be that alcohol dependence results in a redistribution of inputs across OFC excitatory and inhibitory populations and/or alters input transmission onto OFC circuits, thereby altering their ability to contribute to decision-making.

As with all brain areas, the capacity to contribute to decision-making computations is going to depend on the afferent inputs as well as local capabilities. Alcohol dependence is likely to affect both across the brain. Here we identified some of the complexity in how OFC's contributions to decision-making computations are altered following alcohol dependence. These findings will hopefully shed light on the behavioral and OFC-based perturbations previously reported and provide needed insight into the therapeutic treatment of alcohol dependence.

Materials and Methods

Animals

Male and female C57BL/6J mice (n = 15, 9 males, 6 females for non-recording experiments; n = 18, 17 males, 1 female for recording experiments) were housed 2–5 per cage under a 14/10 hour light/dark cycle with access to food (Labdiet 5015) and water ad libitum unless stated otherwise. C57BL/6J (The Jackson Laboratory, Bar Harbor, ME, USA) mice were at least 6 weeks of age prior to intracranial micro-array implant and at least 52 days of age prior to vapor procedures or behavioral training. Investigators were not blind to the experimental groups. The Animal Care and Use Committee of the University of California, San Diego approved all experiments and experiments were conducted according to the NIH guidelines.

Surgical Procedures

Animals under isoflurane anesthesia were implanted with a stereotaxically guided fixed micro-array consisting of four-rows of four platinum-plated tungsten electrodes (35 µm tip, Innovative Neurophysiology, Durham, NC, USA), with electrodes spaced 150 µm apart, and rows 150 µm apart. To maximize targeting of the OFC, arrays were centered at the following coordinates from bregma: A, 2.5 mm; M/L, 1.3 mm; V, 2.0 mm. An additional

bilateral craniotomy was made over the posterior cerebellum for placement of screws wrapped with the electrical reference wire attached to the micro-array. After testing, mice were euthanized, and brains extracted and fixed in 4% paraformaldehyde. Micro-array placement was qualified by examining tracts in 50–100 μm thick brain slices under a macro fluorescence microscope (Olympus MVX10). A subset of micro-arrays was dyed with a 25 mg/ml DiI (1,1′-Dioctadecyl-3,3,3′,3′-tetramethylindocarbocyanine perchlorate) solution in 200 proof ethanol (Sigma) for placement verification. All surgical and behavioral experiments were performed during the light portion of the cycle.

Chronic Intermittent Ethanol Exposure and repeated withdrawal

One to two weeks after micro-array implant surgeries for recording mice, all mice were exposed to four rounds of ethanol vapor or air (H. C. Becker & Hale, 1993; Howard C. Becker & Lopez, 2004; Marcelo F. Lopez & Becker, 2005; Griffin et al., 2009; Renteria et al., 2018). Each round consisted of 16 hours of vapor exposure followed by an 8-hour withdrawal period, repeated for 4 consecutive days. The CIE procedure is designed to repeatedly induce alcohol withdrawal syndrome after long periods of alcohol exposure, a key criterion in the diagnosis of alcohol dependence (Marcelo F. Lopez & Becker, 2005). Ethanol was volatilized by bubbling air through a flask containing 95% ethanol at a rate of 2–3 L/min. The resulting ethanol vapor was combined with a separate air stream to give a total flow rate of approximately 10 L/min, which was delivered to the mice housed in Plexiglas chambers (Plas Labs Inc). Mice were not pre-treated with a loading dose of ethanol or pyrazole to avoid confounding effects of stress that can bias reliance on habitual control, as well as to avoid the effects of pyrazole on neural activity, including actions at the N-methy-D-aspartate (NMDA) receptor (Pereira et al., 1992; Howard C. Becker & Lopez, 2004; Dias-Ferreira et al., 2009). Blood ethanol concentrations (BEC) were collected at the end of each round from separate, non-experimental mice to avoid previously reported stress effects on decision-making from blood extraction on Air mice (mean ± SEM BEC = 29.53 ± 2.36 mM). BEC assays that experienced technical errors were excluded from this measurement.

Behavioral Task

We adapted a lever press hold down task previously used to assay the timing of decision-making actions in mice (Yin, 2009; Fan et al., 2012). Mice were trained in standard operant chambers with one lever extended to the left (or right) of a food magazine and a house light on the opposite wall within sound-attenuating boxes (Med-Associates). Two days before training, mice were food restricted and maintained at 85%-90% of their baseline body weight throughout training and testing.

Magazine training

On the first day, mice were trained to retrieve pellets from the food magazine (no levers present) on a random time (RT) schedule, with a pellet outcome delivered on average every 120 seconds for 60 min.

Continuous reinforcement

The next 3 days the left (or right) lever was present the entire duration of the session. Lever presses were rewarded on a continuous reinforcement (CRF) schedule for up to 15 (CRF day 1), 30 (CRF day 2), or 60 (CRF day 3) pellet deliveries or until 60–90 minutes had passed. For electrode-implanted animals, an additional CRF training day (4 days total) was administered with the implant connected to the amplifier board to habituate the animal to the tethered connection.

Lever Press Hold Down Training

The action differentiation task required lever press durations to exceed a duration criterion assigned prior to the start of the daily session. This criterion was the minimum duration of time the animal was required to hold the lever in a depressed position to receive a reward. Each session began with the house light turning on and the left (or right) lever being extended for the duration of the session. Lever pressing was self-initiated and self-paced without an imposed trial structure (i.e. the lever was never retracted until the session was complete). Reward delivery occurred at the offset of the lever press only if the hold down timer exceeded the session's assigned duration criterion. Sessions were completed when 30 outcomes (non-recording animals) or 60 outcomes (recording animals) were earned or after 90 minutes, whichever came first. The lever press duration

criterion for the first 5 days was 800 milliseconds, followed by 5 days (4 days in 3 animals due to head-cap implant falling off) of a lever press duration requirement of 1600 milliseconds.

Devaluation Testing

Following the last day of hold down testing in the behavioral cohort, mice were habituated to a novel cage and 20% sucrose solution for an hour each. Devaluation testing through sensory-specific satiation was conducted across 2 days and consisted of a valued day and a devalued day. For the valued day, the mice were allowed to pre-feed for 1 hour on 20% sucrose solution. For the devalued day, mice could pre-feed for 1 hour on the pellet outcome previously earned in the lever press hold down task. Mice that did not consume enough pellets (> 0.1 grams) or sucrose (> 0.1 ml) during pre-feeding were excluded from subsequent analysis. Each day immediately following pre-feeding, mice were placed into their respective operant chamber for 10 min where the number and duration of lever presses made were recorded, but no outcome was delivered. Investigators were not blind to the experimental groups. Valued and Devalued days were counterbalanced and run across consecutive days.

Electrophysiological Recordings and Spike Sorting.

Spike activity and local field potentials were recorded using an RHD2000 USB interface board system connected to an amplifier board via a serial peripheral interface (SPI) cable (Intan Technologies, Los Angeles, CA, USA). Electrode signals were amplified, digitized at 30 kHz and filtered between 0.1 Hz and 6 kHz for spikes and 0.1 Hz and 600 Hz for local field potentials. Initial sorting occurred prior to each testing session using an online-sorting algorithm (OpenEphys(Siegle et al., 2017)). Behavior events that occurred inside the operant boxes were timestamped in synchronization in OpenEphys with neural activity using TTL pulses collected at a 10 ms resolution from Med Associates SuperPort Output cards. Spike data was re-sorted offline (Offline Sorter, Plexon, Inc.) using a T-Distribution Expectation-Maximization Scan algorithm in 3D feature space (Shoham et al., 2003). This allowed for the identification of neuronal activity units based on waveform, amplitude, and inter spike interval histogram (no spikes during a refractory period of 1.4 ms). After sorting, each isolated cluster of waveforms was then manually inspected, and biologically implausible waveform

clusters were removed from further analysis. To ensure high signal-to-noise quality of each waveform cluster, waveforms 2 standard deviations greater than the clustered population mean were excluded from the analyses. Units with < 1,000 spike waveforms captured within an entire recording session or that did not show consistent activity across a recording session were not included in our analyses.

Identification of Significantly Modulated Units

To initially examine task-related neural activity, for each previously isolated recorded unit we constructed a peri-event histogram (PETH) around time-stamped lever-press and reward delivery events, such that neural activity was binned into 20-ms bins and averaged across events to analyze amplitude and latency during the recorded behaviors. Per-unit PETHs were then smoothed using a Gaussian-weighted moving average over three bins (60 ms). Using the distribution of the PETH from 10,000 to 2,000 ms before lever press onset as baseline activity, we focused our analysis on a period 2,000 ms before to 10,000 ms after task-related events. A task-related neuron was up-modulated if it had a significant increase in firing rate defined as at least 4 bins (80 ms) with a firing rate larger than a threshold of 95% confidence interval above baseline (-5 to -2 seconds prior to lever press onset) activity during the period from 2,000 before to 3,000 ms after each task event. A task-related neuron was down-modulated if it had a significant decrease in firing rate if at least 4 consecutive bins (80 ms) had a firing rate smaller than a threshold of 95% confidence interval below baseline activity during the period from 2,000 before to 3,000 ms after each task event (Jin & Costa, 2010). The onset of significantly modulated task-related activity was defined as the first of these four consecutive significant PETH bins.

Population Analyses

Performance-related spike activity

To investigate differences in peri-event spike activity between lever presses that were rewarded or not, spike timestamps occurring 10,000 ms before to 10,000 ms after individual lever press events were split into successes (lever press duration exceeded session's criterion duration) and failures (lever press duration did not exceed session's criterion duration). Performance segmented neural activity was then binned into 20-ms bins, averaged across events, and then smoothed using a Gaussian-weighted moving average over three bins

(60 ms), resulting in two PETHs per unit (successes or failures). Individual PETHs were then converted to z-scores using the mean and standard deviation of the firing rate during a baseline period occurring 10,000 to 2,000 before lever press onset. Per-unit Z-scored PETHs were then averaged by treatment group to construct population response profiles for each group. Population spike activity was further segmented into a timepoint late in training (days 4 and 5 of 1600-ms duration criterion), such that a minimum of one session per animal was included. Population spike activity traces were then smoothed with Matlab's Savitzky-Golay *smoothdata* method using a 400 sample sliding window for visual display purposes only.

Ongoing lever press-related spike activity

To investigate differences in spike activity during ongoing lever-presses, each lever press duration was first calculated by subtracting the lever press onset timestamps from lever press offset timestamps. Each lever press duration was then segmented into four equivalent proportion bins (0-25%, 25-50%, 50-75%, 75-100% of lever press duration), and all spikes occurring within each of these duration bins were counted and calculated as a proportion of all spikes that occurred during that lever press.

Duration-related spike activity

To investigate differences in peri-event spike activity between different lever press durations, spike timestamps occurring 10,000 ms before to 10,000 ms after individual lever press events were segmented into four quartiles determined by the distribution of lever press durations within each individual recording session. Duration quartile-segmented neural activity was then binned into 20-ms bins, averaged across events, and then smoothed using a Gaussian-weighted moving average over three bins (60 ms), resulting in four PETHs per unit, one for each quartile. To account for variable lever press durations, individual PETHs were then converted to z-scores using the mean and standard deviation of the firing rate during a pre-lever press onset baseline period that was proportionate to the average lever press duration within each quartile. Per-unit Z-scored PETHs were then averaged by treatment group and quartile groups to construct population response profiles.

Neural decoding of task performance from spike activity

For all units from recording sessions in which a minimum of 10 lever presses exceeded the session's lever press duration criterion, spike timestamps occurring 2,000 ms before to 10,000 ms after individual lever press events were binned into 1-ms bins and labeled by lever press outcome (success or failure to exceed the session's lever press duration criterion). These peri-event rasters were then segmented by treatment groups and lever press event type (onset or offset) and used to train a model to classify successful lever presses. The classifier, a support vector machine model implemented in Matlab with the NDT toolbox, was trained and tested at 100 ms steps with a bin width of 200 ms (Meyers, 2013). For each of these time points, the classifier used 10 cross-validation splits to segment per-unit firing rates from randomly selected lever press events into training (90%) and testing (10%) sets for 500 resampling runs. Significance at each of these timepoints was tested by first creating 5 null distributions of decoding accuracy with 500 resampling runs each in which the performance labels were shuffled. The accuracy of our decoder was then compared to these null distributions across all time points.

Statistical Procedures

Statistical significance was defined as an alpha of $p < 0.05$. Statistical analysis was performed using GraphPad Prism 8.3.0 (GraphPad Software) and custom MATLAB R2019a (MathWorks) scripts (https://github.com/gremellab/CIEOFCHOLD). Acquisition data, including lever presses, response rate, and proportion of lever presses that were rewarded were analyzed using two-way repeated measures ANOVA (Session x Treatment) unless otherwise noted. For outcome devaluation testing, two-way repeated measure ANOVAs (State × Treatment) with post-hoc Sidak's multiple comparison testing were performed to examine differences in the patterns of responding. For peri-event spike activity comparisons, per-unit average z-scored firing rates were binned into four 250-ms bins before the lever press onset, or after lever press offset and after reward delivery, respectively. Within treatment groups, we performed two-way repeated measure ANOVAs (Bin × Outcome) to examine differences in spike activity between lever presses that failed or succeeded to exceed the session's lever press duration criteria, with post-hoc Sidak's multiple comparison testing to determine bins in which differences were pronounced. Two-way repeated measure ANOVAs (Bin × Treatment) were performed to examine differences in spike activity between treatment groups, with post-hoc Sidak's

multiple comparison testing to determine bins in which differences were pronounced. For within-treatment group comparisons of activity between lever press duration quartiles, ordinary one-way ANOVAs (Quartile) were performed on the average z-scored firing rate of the window of interest, with post-hoc Sidak's multiple comparison testing used to determine quartiles in which differences were pronounced. For only this analysis, one unit in the up-modulated population group was excluded as an outlier (> 20 z-score value in first segment). Two-way repeated measure ANOVAs (Segment × Treatment) were performed to examine group differences in the proportions of spikes occurring between lever press duration segments. When appropriate, mixed-effect analyses were conducted in lieu of repeated measures ANOVAs (e.g. when data points were missing due to loss of implant). Data are presented as mean ± SEM.

Key Resources Table

Reagent type (species) or resource	Designation	Source or reference	Identifiers	Additional information
Software, algorithm	MATLAB	this paper	RRID:SCR_001622	https://github.com/gremellab/lickingstructure;
Software, algorithm	MED-PC IV Software Suite	Med Associates	RRID:SCR_012156	
Software, algorithm	Arduino	this paper		https://github.com/gremellab/arduinoLEDcontrol;
Software, algorithm	GraphPad Prism 6	GraphPad	RRID:SCR_002798	
Software, algorithm	Adobe Illustrator CS6	Adobe	RRID:SCR_010279	
Software, algorithm	Open Ephys GUI	Siegle JH, López AC, Patel YA, Abramov K, Ohayon S, Voigts J. Open Ephys: an open-source, plugin-based platform for multichannel electrophysiology. J Neural Eng. 2017;14(4):045003. doi:10.1088/1741-2552/aa5eea		https://github.com/open-ephys/plugin-GUI
Software, algorithm	Neuroexplorer	Nex Technologies	RRID:SCR_001818	
Software, algorithm	Offline Sorter 4.4.0	Plexon	RRID:SCR_000012	

Software, algorithm	The Neural Decoding Toolbox	Meyers, E. (2013). The Neural Decoding Toolbox. Frontiers in Neuroinformatics, 7:8	RRID:SCR_009012	http://www.readout.info/
Software, algorithm	Perceptually Uniform Colormaps	Ander Biguri		https://www.mathworks.com/matlabcentral/fileexchange/51986-perceptually-uniform-colormaps
Software, algorithm	shadedErrorBar	Rob Campbell		https://github.com/raacampbell/shadedErrorBar
Hardware	4x4 Fixed Micro-Array, 35 uM Tungsten Electrodes, 150 uM Electrode Spacing, 150 uM Row Spacing, 4mm Electrode Length, 200 uM Silver Ground Wire	Innovative Neurophysiology, Inc.		
Hardware	RHD2000 USB Interface Board	Intant Technologies		
Hardware	RHD2000 SPI Cables	Intant Technologies		
Hardware	RHD2216 Amplifier Board	Intant Technologies		
Hardware	AM1 Alcohol Analyser	Analox Instruments		
Hardware	Operant chambers	Med-Associates	MED-307W-D1	
Hardware	Custom vapor chambers	Plas Labs Inc.		
Chemical compound, dye	1,1′-Dioctadecyl-3,3,3′,3′-tetramethylindocarbocyanine perchlorate	MilliporeSigma	468495	
Chemical compound, ethanol	Koptec Pure Ethanol – 190 Proof	Decon Labs Inc.		

Acknowledgements

This research was supported by R00AA021780, R01AA026077, Whitehall and Brain and Behavior Foundations to C.MG, and NSF GRFP grant number DGE-1650112 to C.C. We thank undergraduate research assistant Mariela Lopez Valencia for the technical assistance and Roy Jungay for animal care assistance.

Competing Interests

The authors express no financial and non-financial competing interests.

References

American Psychological Association. (2013). *Diagnostic and Statistical Manual of Mental Disorders (DSM-5®)*. American Psychiatric Pub.

Badanich, K. A., Becker, H. C., & Woodward, J. J. (2011). Effects of chronic intermittent ethanol exposure on orbitofrontal and medial prefrontal cortex-dependent behaviors in mice. *Behavioral Neuroscience*, *125*(6), 879–891. https://doi.org/10.1037/a0025922

Badanich, K. A., Mulholland, P. J., Beckley, J. T., Trantham-Davidson, H., & Woodward, J. J. (2013). Ethanol Reduces Neuronal Excitability of Lateral Orbitofrontal Cortex Neurons Via a Glycine Receptor Dependent Mechanism. *Neuropsychopharmacology*, *38*(7), 1176–1188. https://doi.org/10.1038/npp.2013.12

Baltz, E. T., Yalcinbas, E. A., Renteria, R., & Gremel, C. M. (2018). Orbital frontal cortex updates state-induced value change for decision-making. *ELife*, *7*. https://doi.org/10.7554/eLife.35988

Beck, A., Wüstenberg, T., Genauck, A., Wrase, J., Schlagenhauf, F., Smolka, M. N., Mann, K., & Heinz, A. (2012). Effect of Brain Structure, Brain Function, and Brain Connectivity on Relapse in Alcohol-Dependent Patients. *Archives of General Psychiatry*, *69*(8), 842–852. https://doi.org/10.1001/archgenpsychiatry.2011.2026

Becker, H. C., & Hale, R. L. (1993). Repeated episodes of ethanol withdrawal potentiate the severity of subsequent withdrawal seizures: An animal model of alcohol withdrawal “kindling.” *Alcoholism, Clinical and Experimental Research*, *17*(1), 94–98. https://doi.org/10.1111/j.1530-0277.1993.tb00731.x

Becker, Howard C., & Lopez, M. F. (2004). Increased ethanol drinking after repeated chronic ethanol exposure and withdrawal experience in C57BL/6 mice. *Alcoholism, Clinical and Experimental Research*, *28*(12), 1829–1838.

Berre, A.-P. L., Vabret, F., Cauvin, C., Pinon, K., Allain, P., Pitel, A.-L., Eustache, F., & Beaunieux, H. (2012). Cognitive Barriers to Readiness to Change in Alcohol-Dependent Patients. *Alcoholism: Clinical and Experimental Research*, *36*(9), 1542–1549. https://doi.org/10.1111/j.1530-0277.2012.01760.x

Bickel, W. K., Mellis, A. M., Snider, S. E., Athamneh, L. N., Stein, J. S., & Pope, D. A. (2018). 21st century neurobehavioral theories of decision making in addiction: Review and evaluation. *Pharmacology Biochemistry and Behavior*, *164*, 4–21. https://doi.org/10.1016/j.pbb.2017.09.009

Boettiger, C. A., Mitchell, J. M., Tavares, V. C., Robertson, M., Joslyn, G., D'Esposito, M., & Fields, H. L. (2007). Immediate Reward Bias in Humans: Fronto-Parietal Networks and a Role for the Catechol-O-Methyltransferase 158Val/Val Genotype. *Journal of Neuroscience*, *27*(52), 14383–14391. https://doi.org/10.1523/JNEUROSCI.2551-07.2007

Cardenas, V. A., Durazzo, T. C., Gazdzinski, S., Mon, A., Studholme, C., & Meyerhoff, D. J. (2011). Brain morphology at entry into treatment for alcohol dependence is related to relapse propensity. *Biological Psychiatry*, *70*(6), 561–567. https://doi.org/10.1016/j.biopsych.2011.04.003

Chanraud, S., Martelli, C., Delain, F., Kostogianni, N., Douaud, G., Aubin, H.-J., Reynaud, M., & Martinot, J.-L. (2007). Brain Morphometry and Cognitive Performance in Detoxified Alcohol-Dependents with Preserved Psychosocial Functioning. *Neuropsychopharmacology*, *32*(2), 429–438. https://doi.org/10.1038/sj.npp.1301219

Dias-Ferreira, E., Sousa, J. C., Melo, I., Morgado, P., Mesquita, A. R., Cerqueira, J. J., Costa, R. M., & Sousa, N. (2009). Chronic stress causes frontostriatal reorganization and affects decision-making. *Science (New York, N.Y.)*, *325*(5940), 621–625. https://doi.org/10.1126/science.1171203

Dickinson, A. (1985). Actions and Habits: The Development of Behavioural Autonomy. *Philosophical Transactions of the Royal Society of London Series B*, *308*, 67. https://doi.org/10.1098/rstb.1985.0010

Durazzo, T. C., Tosun, D., Buckley, S., Gazdzinski, S., Mon, A., Fryer, S. L., & Meyerhoff, D. J. (2011). Cortical thickness, surface area, and volume of the brain reward system in alcohol dependence: Relationships to relapse and extended abstinence. *Alcoholism, Clinical and Experimental Research*, *35*(6), 1187–1200. https://doi.org/10.1111/j.1530-0277.2011.01452.x

Ernst, L. H., Plichta, M. M., Dresler, T., Zesewitz, A. K., Tupak, S. V., Haeussinger, F. B., Fischer, M., Polak, T., Fallgatter, A. J., & Ehlis, A.-C. (2014). Prefrontal correlates of approach preferences for alcohol stimuli in alcohol dependence. *Addiction Biology*, *19*(3), 497–508. https://doi.org/10.1111/adb.12005

Fan, D., Rossi, M. A., & Yin, H. H. (2012). Mechanisms of action selection and timing in substantia nigra neurons. *The Journal of Neuroscience: The Official Journal of the Society for Neuroscience*, *32*(16), 5534–5548. https://doi.org/10.1523/JNEUROSCI.5924-11.2012

Fellows, L. K. (2007). The role of orbitofrontal cortex in decision making: A component process account. *Annals of the New York Academy of Sciences*, *1121*, 421–430. https://doi.org/10.1196/annals.1401.023

Fernandez, G. M., Lew, B. J., Vedder, L. C., & Savage, L. M. (2017). Chronic intermittent ethanol exposure leads to alterations in brain-derived neurotrophic factor within the frontal cortex and impaired behavioral flexibility in both adolescent and adult rats. *Neuroscience*, *348*, 324–334. https://doi.org/10.1016/j.neuroscience.2017.02.045

Gourley, S. L., Olevska, A., Zimmermann, K. S., Ressler, K. J., DiLeone, R. J., & Taylor, J. R. (2013). The orbitofrontal cortex regulates outcome-based decision-making via the lateral striatum. *The European Journal of Neuroscience*, *38*(3). https://doi.org/10.1111/ejn.12239

Gremel, C. M., Chancey, J. H., Atwood, B. K., Luo, G., Neve, R., Ramakrishnan, C., Deisseroth, K., Lovinger, D. M., & Costa, R. M. (2016). Endocannabinoid Modulation of Orbitostriatal Circuits Gates Habit Formation. *Neuron*, *90*(6), 1312–1324. https://doi.org/10.1016/j.neuron.2016.04.043

Gremel, C. M., & Costa, R. M. (2013). Orbitofrontal and striatal circuits dynamically encode the shift between goal-directed and habitual actions. *Nature Communications*, *4*, 2264. https://doi.org/10.1038/ncomms3264

Griffin, W. C., Lopez, M. F., & Becker, H. C. (2009). Intensity and duration of chronic ethanol exposure is critical for subsequent escalation of voluntary ethanol drinking in mice. *Alcoholism, Clinical and Experimental Research*, *33*(11), 1893–1900. https://doi.org/10.1111/j.1530-0277.2009.01027.x

Hermann, D., Smolka, M. N., Wrase, J., Klein, S., Nikitopoulos, J., Georgi, A., Braus, D. F., Flor, H., Mann, K., & Heinz, A. (2006). Blockade of cue-induced brain activation of abstinent alcoholics by a single administration of amisulpride as measured with fMRI. *Alcoholism, Clinical and Experimental Research*, *30*(8), 1349–1354. https://doi.org/10.1111/j.1530-0277.2006.00174.x

Jin, X., & Costa, R. M. (2010). Start/Stop Signals Emerge in Nigrostriatal Circuits during Sequence Learning. *Nature*, *466*(7305), 457–462. https://doi.org/10.1038/nature09263

Jones, J. L., Esber, G. R., McDannald, M. A., Gruber, A. J., Hernandez, A., Mirenzi, A., & Schoenbaum, G. (2012). Orbitofrontal cortex supports behavior and learning using inferred but not cached values. *Science (New York, N.Y.)*, *338*(6109), 953–956. https://doi.org/10.1126/science.1227489

Kepecs, A., Uchida, N., Zariwala, H. A., & Mainen, Z. F. (2008). Neural correlates, computation and behavioural impact of decision confidence. *Nature*, *455*(7210), 227–231. https://doi.org/10.1038/nature07200

Kroener, S., Mulholland, P. J., New, N. N., Gass, J. T., Becker, H. C., & Chandler, L. J. (2012). Chronic Alcohol Exposure Alters Behavioral and Synaptic Plasticity of the Rodent Prefrontal Cortex. *PLOS ONE*, *7*(5), e37541. https://doi.org/10.1371/journal.pone.0037541

Kuch, D. O. (1974). Differentiation of Press Durations with Upper and Lower Limits on Reinforced Values. *Journal of the Experimental Analysis of Behavior*, *22*(2), 275–283. https://doi.org/10.1901/jeab.1974.22-275

Laakso, M. P., Gunning-Dixon, F., Vaurio, O., Repo-Tiihonen, E., Soininen, H., & Tiihonen, J. (2002). Prefrontal volumes in habitually violent subjects with antisocial personality disorder and type 2 alcoholism. *Psychiatry Research*, *114*(2), 95–102. https://doi.org/10.1016/s0925-4927(02)00005-7

Le Berre, A.-P., Fama, R., & Sullivan, E. V. (2017). Executive Functions, Memory, and Social Cognitive Deficits and Recovery in Chronic Alcoholism: A Critical Review to Inform Future Research. *Alcoholism, Clinical and Experimental Research*, *41*(8), 1432–1443. https://doi.org/10.1111/acer.13431

Loeber, S., Duka, T., Welzel, H., Nakovics, H., Heinz, A., Flor, H., & Mann, K. (2009). Impairment of Cognitive Abilities and Decision Making after Chronic Use of Alcohol: The Impact of Multiple Detoxifications. *Alcohol and Alcoholism*, *44*(4), 372–381. https://doi.org/10.1093/alcalc/agp030

Lopez, M. F., Becker, H. C., & Chandler, L. J. (2014). Repeated episodes of chronic intermittent ethanol promote insensitivity to devaluation of the reinforcing effect of ethanol. *Alcohol (Fayetteville, N.Y.)*, *48*(7), 639–645. https://doi.org/10.1016/j.alcohol.2014.09.002

Lopez, Marcelo F., & Becker, H. C. (2005). Effect of pattern and number of chronic ethanol exposures on subsequent voluntary ethanol intake in C57BL/6J mice. *Psychopharmacology*, *181*(4), 688–696. https://doi.org/10.1007/s00213-005-0026-3

Lüscher, C., Robbins, T. W., & Everitt, B. J. (2020). The transition to compulsion in addiction. *Nature Reviews Neuroscience*, *21*(5), 247–263. https://doi.org/10.1038/s41583-020-0289-z

Malvaez, M., Shieh, C., Murphy, M. D., Greenfield, V. Y., & Wassum, K. M. (2019). Distinct cortical–amygdala projections drive reward value encoding and retrieval. *Nature Neuroscience*, *22*(5), 762–769. https://doi.org/10.1038/s41593-019-0374-7

Masset, P., Ott, T., Lak, A., Hirokawa, J., & Kepecs, A. (2020). Behavior- and Modality-General Representation of Confidence in Orbitofrontal Cortex. *Cell*, *0*(0). https://doi.org/10.1016/j.cell.2020.05.022

McGuier, N. S., Padula, A. E., Lopez, M. F., Woodward, J. J., & Mulholland, P. J. (2015). Withdrawal from chronic intermittent alcohol exposure increases dendritic spine density in the lateral orbitofrontal cortex of mice. *Alcohol*, *49*(1), 21–27. https://doi.org/10.1016/j.alcohol.2014.07.017

Meyers, E. M. (2013). The neural decoding toolbox. *Frontiers in Neuroinformatics*, *7*. https://doi.org/10.3389/fninf.2013.00008

Milad, M. R., & Rauch, S. L. (2012). Obsessive-compulsive disorder: Beyond segregated cortico-striatal pathways. *Trends in Cognitive Sciences*, *16*(1), 43–51. https://doi.org/10.1016/j.tics.2011.11.003

Myrick, H., Anton, R. F., Li, X., Henderson, S., Drobes, D., Voronin, K., & George, M. S. (2004). Differential brain activity in alcoholics and social drinkers to alcohol cues: Relationship to craving. *Neuropsychopharmacology: Official Publication of the American College of Neuropsychopharmacology*, *29*(2), 393–402. https://doi.org/10.1038/sj.npp.1300295

Myrick, H., Anton, R. F., Li, X., Henderson, S., Randall, P. K., & Voronin, K. (2008). Effect of naltrexone and ondansetron on alcohol cue-induced activation of the ventral striatum in alcohol-dependent people. *Archives of General Psychiatry*, *65*(4), 466–475. https://doi.org/10.1001/archpsyc.65.4.466

Nimitvilai, S., Lopez, M. F., Mulholland, P. J., & Woodward, J. J. (2016). Chronic Intermittent Ethanol Exposure Enhances the Excitability and Synaptic Plasticity of Lateral Orbitofrontal Cortex Neurons and Induces a Tolerance to the Acute Inhibitory Actions of Ethanol. *Neuropsychopharmacology*, *41*(4), 1112–1127. https://doi.org/10.1038/npp.2015.250

Nimitvilai, S., Lopez, M. F., Mulholland, P. J., & Woodward, J. J. (2017). Ethanol Dependence Abolishes Monoamine and GIRK (Kir3) Channel Inhibition of Orbitofrontal Cortex Excitability.

Neuropsychopharmacology: Official Publication of the American College of Neuropsychopharmacology, *42*(9), 1800–1812. https://doi.org/10.1038/npp.2017.22

Nimitvilai, S., Uys, J. D., Woodward, J. J., Randall, P. K., Ball, L. E., Williams, R. W., Jones, B. C., Lu, L., Grant, K. A., & Mulholland, P. J. (2017). Orbitofrontal Neuroadaptations and Cross-Species Synaptic Biomarkers in Heavy-Drinking Macaques. *The Journal of Neuroscience: The Official Journal of the Society for Neuroscience*, *37*(13), 3646–3660. https://doi.org/10.1523/JNEUROSCI.0133-17.2017

Niv, Y. (2019). Learning task-state representations. *Nature Neuroscience*, *22*(10), 1544–1553. https://doi.org/10.1038/s41593-019-0470-8

Padoa-Schioppa, C., & Conen, K. E. (2017). Orbitofrontal Cortex: A Neural Circuit for Economic Decisions. *Neuron*, *96*(4), 736–754. https://doi.org/10.1016/j.neuron.2017.09.031

Pauls, D. L., Abramovitch, A., Rauch, S. L., & Geller, D. A. (2014). Obsessive-compulsive disorder: An integrative genetic and neurobiological perspective. *Nature Reviews. Neuroscience*, *15*(6), 410–424. https://doi.org/10.1038/nrn3746

Pereira, E. F., Aracava, Y., Aronstam, R. S., Barreiro, E. J., & Albuquerque, E. X. (1992). Pyrazole, an alcohol dehydrogenase inhibitor, has dual effects on N-methyl-D-aspartate receptors of hippocampal pyramidal cells: Agonist and noncompetitive antagonist. *The Journal of Pharmacology and Experimental Therapeutics*, *261*(1), 331–340.

Platt, J. R., Kuch, D. O., & Bitgood, S. C. (1973). Rats' Lever-Press Durations as Psychophysical Judgments of Time1. *Journal of the Experimental Analysis of Behavior*, *19*(2), 239–250. https://doi.org/10.1901/jeab.1973.19-239

Reich, R. R., & Goldman, M. S. (2015). Decision making about alcohol use: The case for scientific convergence. *Addictive Behaviors*, *44*, 23–28. https://doi.org/10.1016/j.addbeh.2014.12.001

Reinhard, I., Leménager, T., Fauth-Bühler, M., Hermann, D., Hoffmann, S., Heinz, A., Kiefer, F., Smolka, M. N., Wellek, S., Mann, K., & Vollstädt-Klein, S. (2015). A comparison of region-of-interest measures for extracting whole brain data using survival analysis in alcoholism as an example. *Journal of Neuroscience Methods*, *242*, 58–64. https://doi.org/10.1016/j.jneumeth.2015.01.001

Reiter, A. M. F., Deserno, L., Kallert, T., Heinze, H.-J., Heinz, A., & Schlagenhauf, F. (2016). Behavioral and Neural Signatures of Reduced Updating of Alternative Options in Alcohol-Dependent Patients during Flexible Decision-Making. *The Journal of Neuroscience*, *36*(43), 10935–10948. https://doi.org/10.1523/JNEUROSCI.4322-15.2016

Renteria, R., Baltz, E. T., & Gremel, C. M. (2018). Chronic alcohol exposure disrupts top-down control over basal ganglia action selection to produce habits. *Nature Communications*, *9*(1), 211. https://doi.org/10.1038/s41467-017-02615-9

Renteria, R., Cazares, C., & Gremel, C. M. (2020). Habitual Ethanol Seeking and Licking Microstructure of Enhanced Ethanol Self-Administration in Ethanol-Dependent Mice. *Alcoholism: Clinical and Experimental Research*, *44*(4), 880–891. https://doi.org/10.1111/acer.14302

Rhodes, S. E. V., & Murray, E. A. (2013). Differential Effects of Amygdala, Orbital Prefrontal Cortex, and Prelimbic Cortex Lesions on Goal-Directed Behavior in Rhesus Macaques. *The Journal of Neuroscience*, *33*(8), 3380–3389. https://doi.org/10.1523/JNEUROSCI.4374-12.2013

Robbins, T. W., Vaghi, M. M., & Banca, P. (2019). Obsessive-Compulsive Disorder: Puzzles and Prospects. *Neuron*, *102*(1), 27–47. https://doi.org/10.1016/j.neuron.2019.01.046

Schuck, N. W., Cai, M. B., Wilson, R. C., & Niv, Y. (2016). Human Orbitofrontal Cortex Represents a Cognitive Map of State Space. *Neuron*, *91*(6), 1402–1412. https://doi.org/10.1016/j.neuron.2016.08.019

Sebold, M., Nebe, S., Garbusow, M., Guggenmos, M., Schad, D. J., Beck, A., Kuitunen-Paul, S., Sommer, C., Frank, R., Neu, P., Zimmermann, U. S., Rapp, M. A., Smolka, M. N., Huys, Q. J. M., Schlagenhauf, F., & Heinz, A. (2017). When Habits Are Dangerous: Alcohol Expectancies and Habitual Decision Making Predict Relapse in Alcohol Dependence. *Biological Psychiatry*, *82*(11), 847–856. https://doi.org/10.1016/j.biopsych.2017.04.019

Shoham, S., Fellows, M. R., & Normann, R. A. (2003). Robust, automatic spike sorting using mixtures of multivariate t-distributions. *Journal of Neuroscience Methods*, *127*(2), 111–122. https://doi.org/10.1016/S0165-0270(03)00120-1

Siegle, J. H., López, A. C., Patel, Y. A., Abramov, K., Ohayon, S., & Voigts, J. (2017). Open Ephys: An open-source, plugin-based platform for multichannel electrophysiology. *Journal of Neural Engineering*, *14*(4), 045003. https://doi.org/10.1088/1741-2552/aa5eea

Sjoerds, Z., de Wit, S., van den Brink, W., Robbins, T. W., Beekman, A. T. F., Penninx, B. W. J. H., & Veltman, D. J. (2013). Behavioral and neuroimaging evidence for overreliance on habit learning in alcohol-dependent patients. *Translational Psychiatry*, *3*, e337. https://doi.org/10.1038/tp.2013.107

Stalnaker, T. A., Cooch, N. K., McDannald, M. A., Liu, T.-L., Wied, H., & Schoenbaum, G. (2014). Orbitofrontal neurons infer the value and identity of predicted outcomes. *Nature Communications*, *5*, 3926. https://doi.org/10.1038/ncomms4926

Stalnaker, T. A., Cooch, N. K., & Schoenbaum, G. (2015). What the orbitofrontal cortex does not do. *Nature Neuroscience*, *18*(5), 620–627. https://doi.org/10.1038/nn.3982

Stalnaker, T. A., Liu, T.-L., Takahashi, Y. K., & Schoenbaum, G. (2018). Orbitofrontal neurons signal reward predictions, not reward prediction errors. *Neurobiology of Learning and Memory*, *153*(Pt B), 137–143. https://doi.org/10.1016/j.nlm.2018.01.013

Stephens, D. N., & Duka, T. (2008). Cognitive and emotional consequences of binge drinking: Role of amygdala and prefrontal cortex. *Philosophical Transactions of the Royal Society B: Biological Sciences*, *363*(1507), 3169–3179. https://doi.org/10.1098/rstb.2008.0097

Tapert, S. F., Cheung, E. H., Brown, G. G., Frank, L. R., Paulus, M. P., Schweinsburg, A. D., Meloy, M. J., & Brown, S. A. (2003). Neural response to alcohol stimuli in adolescents with alcohol use disorder. *Archives of General Psychiatry*, *60*(7), 727–735. https://doi.org/10.1001/archpsyc.60.7.727

Thayer, R. E., Hagerty, S. L., Sabbineni, A., Claus, E. D., Hutchison, K. E., & Weiland, B. J. (2016). Negative and interactive effects of sex, aging, and alcohol abuse on gray matter morphometry. *Human Brain Mapping*, *37*(6), 2276–2292. https://doi.org/10.1002/hbm.23172

Volkow, N. D., Wang, G. J., Hitzemann, R., Fowler, J. S., Overall, J. E., Burr, G., & Wolf, A. P. (1994). Recovery of brain glucose metabolism in detoxified alcoholics. *The American Journal of Psychiatry*, *151*(2), 178–183. https://doi.org/10.1176/ajp.151.2.178

Volkow, N. D., Wang, G. J., Overall, J. E., Hitzemann, R., Fowler, J. S., Pappas, N., Frecska, E., & Piscani, K. (1997). Regional brain metabolic response to lorazepam in alcoholics during early and late alcohol detoxification. *Alcoholism, Clinical and Experimental Research*, *21*(7), 1278–1284.

Wallis, J. D. (2007). Orbitofrontal cortex and its contribution to decision-making. *Annual Review of Neuroscience*, *30*, 31–56. https://doi.org/10.1146/annurev.neuro.30.051606.094334

Wilson, R. C., Takahashi, Y. K., Schoenbaum, G., & Niv, Y. (2014). Orbitofrontal cortex as a cognitive map of task space. *Neuron*, *81*(2), 267–279. https://doi.org/10.1016/j.neuron.2013.11.005

Wrase, J., Grüsser, S. M., Klein, S., Diener, C., Hermann, D., Flor, H., Mann, K., Braus, D. F., & Heinz, A. (2002). Development of alcohol-associated cues and cue-induced brain activation in alcoholics. *European Psychiatry: The Journal of the Association of European Psychiatrists*, *17*(5), 287–291. https://doi.org/10.1016/s0924-9338(02)00676-4

Yin, H. H. (2009). The role of the murine motor cortex in action duration and order. *Frontiers in Integrative Neuroscience*, *3*, 23. https://doi.org/10.3389/neuro.07.023.2009

Zhou, J., Gardner, M. P. H., Stalnaker, T. A., Ramus, S. J., Wikenheiser, A. M., Niv, Y., & Schoenbaum, G. (2019). Rat Orbitofrontal Ensemble Activity Contains Multiplexed but Dissociable Representations of Value and Task Structure in an Odor Sequence Task. *Current Biology: CB*, *29*(6), 897-907.e3. https://doi.org/10.1016/j.cub.2019.01.048

Zinn, S., Stein, R., & Swartzwelder, H. S. (2004). Executive Functioning Early in Abstinence From Alcohol. *Alcoholism: Clinical and Experimental Research*, *28*(9), 1338–1346. https://doi.org/10.1097/01.ALC.0000139814.81811.62

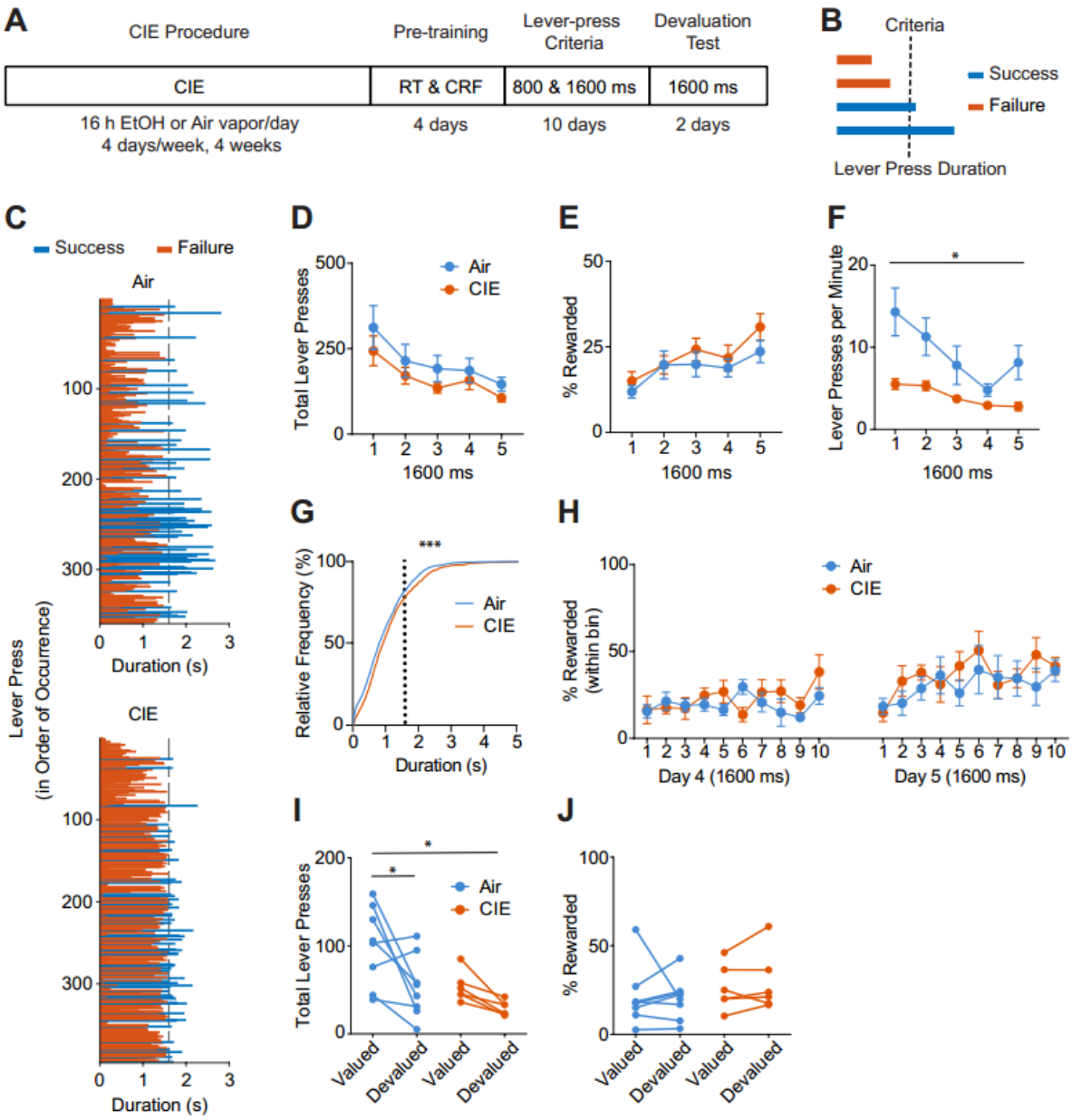

Figure 1. Effects of alcohol dependence on action differentiation and outcome devaluation

(A). Experimental timeline starting with the CIE procedure and subsequent Random Time (RT) and Fixed-Ratio Continuous Reinforcement (CRF) schedules of reinforcement, followed by 5 days of 800-ms lever press duration criterion sessions and 4 to 5 days of 1600-ms lever press duration criterion sessions, and 2 subsequent days of outcome devaluation (DV) testing. **(B).** Schematic of lever press duration performance. Lever presses exceeding the session's minimum hold-down duration criterion were rewarded only at lever press offset. **(C).** Example lever press performance from individual Air and CIE mice occurring within a single 1600-ms hold-down duration criterion session late in training. **(D).** Average total lever presses, **(E)** percentage of rewarded lever presses, and **(F)** lever pressing rate throughout 1600-ms hold down duration criterion sessions. **(G).** Distribution of the relative frequency of lever press durations during the last two days of 1600-ms hold down duration criterion training sessions. **(H).** Average percentage of rewarded lever presses across normalized session duration bins during the last two days of 1600-ms hold down criterion training sessions. **(I).** Total lever presses in Valued and Devalued states throughout DV testing. **(J).** Percentage of successful lever presses in Valued and Devalued states throughout DV testing. Data points represent mean ± SEM. *p<0.05, ***p<0.001.

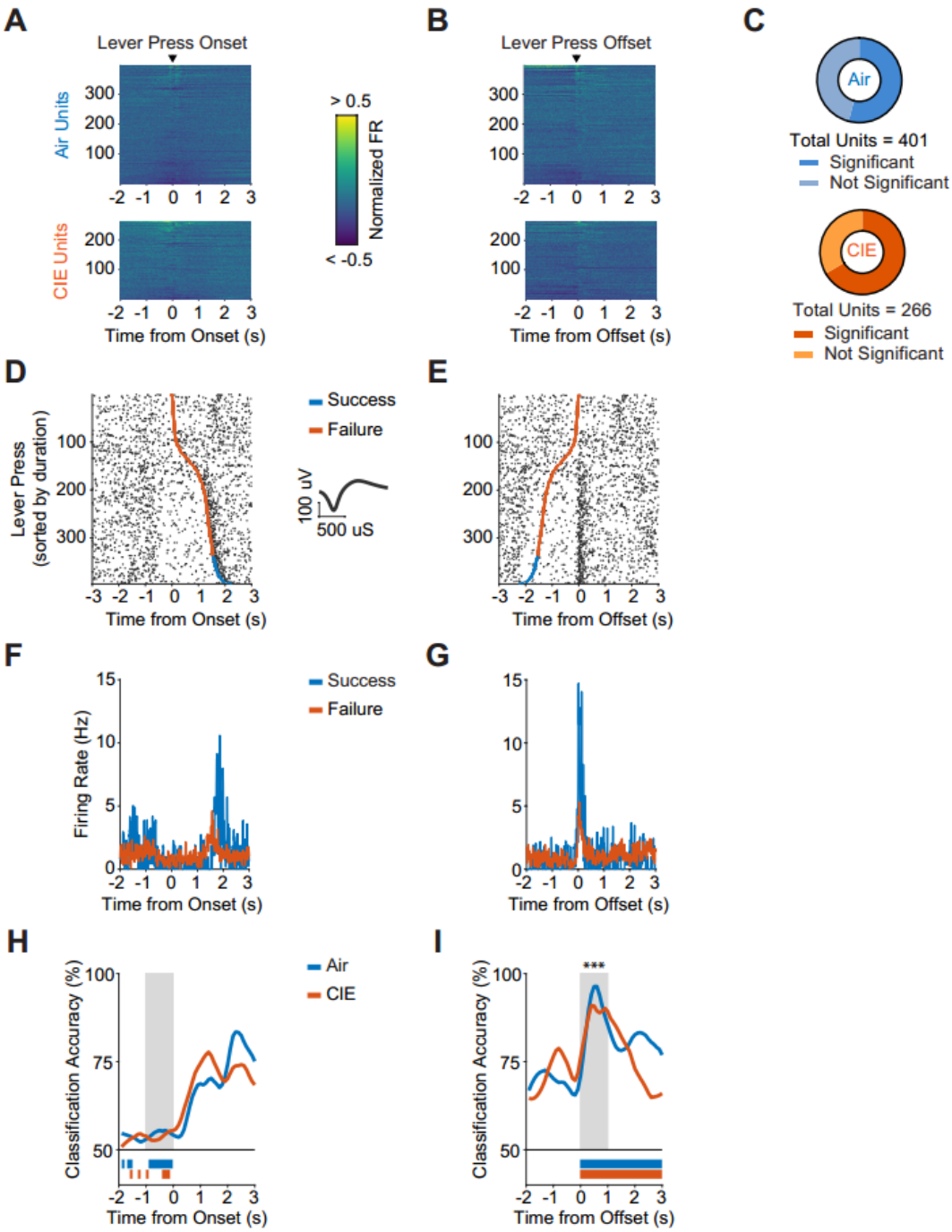

Figure 2. OFC activity represents decision-making success.

(A). Heat map of normalized firing rates for all captured units, relative to lever press onset and **(B)** offset for Air and CIE groups. **(C).** Proportion of all captured units in which firing rates significantly deviated from a baseline period (-5 to -2 seconds before lever press onset) for Air (~54%) and CIE (~66%) groups. **(D)**. Raster plot of a representative unit's firing rate relative to lever press onset and **(E)** offset, sorted from shortest to longest durations within a 1600-ms lever press criterion session that occurred late in training. **(F)**. Representative unit's average firing rates displayed relative to lever press onset and **(G)** offset, segmented by whether a lever press successfully exceeded hold-down criterion (1600-ms) or not. **(H).** SVM classification accuracy of task performance (i.e. lever press successfully exceeded 1600-ms hold-down criterion) from Air and CIE units, relative to lever press onset and **(I)** offset. Bars underneath traces indicate time points in which the accuracy of our decoder was significant compared to the null distribution (-2 to 0 seconds before lever press onset, and 0 to 3 seconds after lever press offset, respectively). Data points represent mean. ***p<0.001.

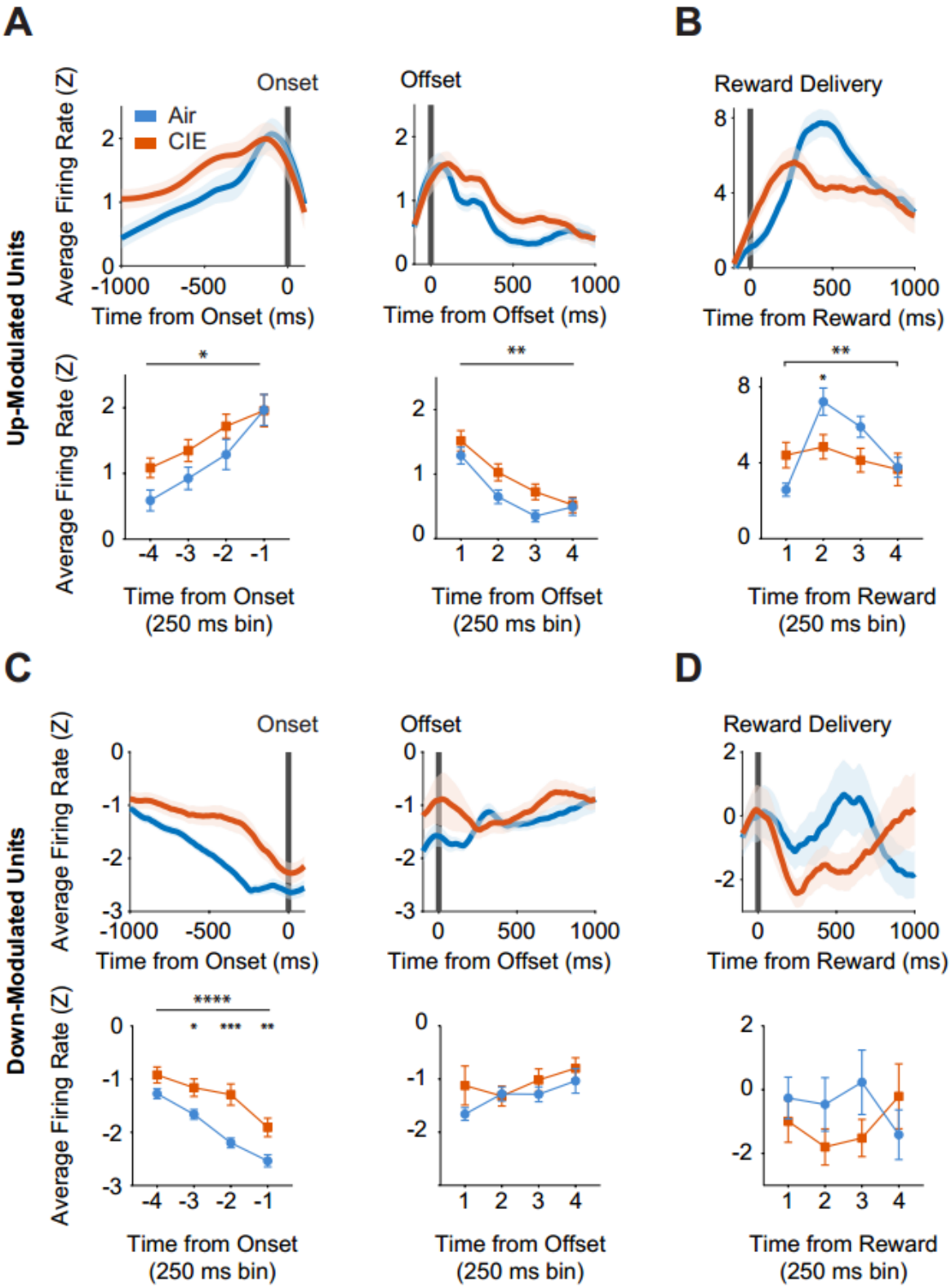

Figure 3. Ethanol dependence alters encoding of inferred decision-making actions and outcomes

(A). Mean z-scored firing rates comprised of all lever presses for significantly up-modulated or **(C)** down-modulated units in Air and CIE animals, relative to lever press onset (top left) and offset (top right). **(B).** Mean z-scored firing rates relative to pellet reward delivery for significantly up-modulated or **(D)** down-modulated units in Air and CIE groups (top). Mean Z-scored firing rates were compared across four 250-ms bins relative to each corresponding task event (A-D bottom). Data points represent mean ± SEM. *p<0.05, **p< 0.01, ***p<0.001, ****p<0.0001.

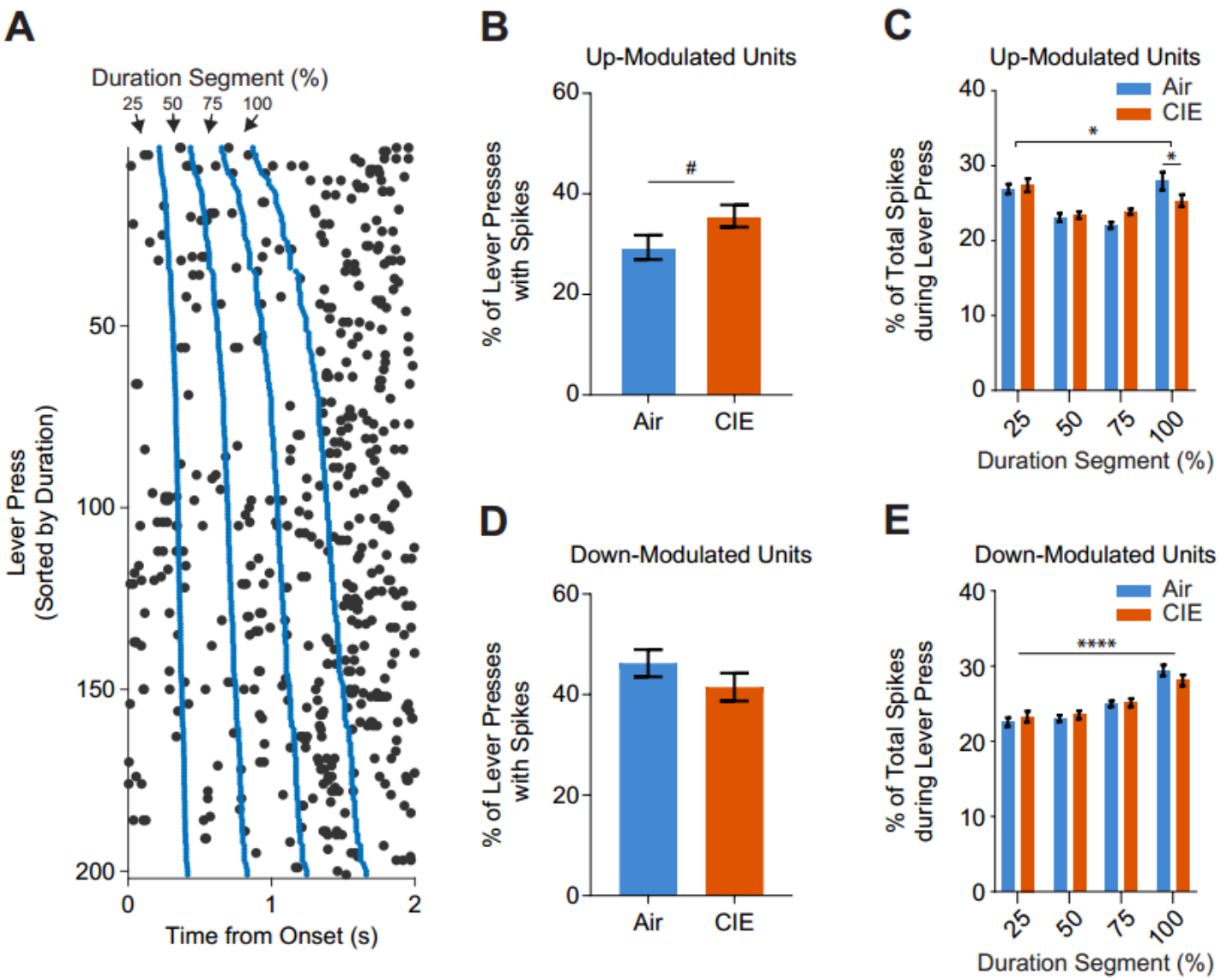

Figure 4. Ethanol dependence alters OFC activity during inferred decision-making

(A). Raster plot of a representative unit's firing rate during lever pressing, relative to lever press onset, sorted from shortest to longest durations within a late 1600-ms lever press criterion session. Blue markers indicate the bin edges of each equidistant lever press duration segment (i.e. 25%, 50%, 75%, 100% of lever press duration). **(B).** Average percentage of lever press durations in which at least one spike occurred for significantly up-modulated and (**D)** down-modulated units in Air and CIE groups. **(C).** Average percentage of total spikes that occurred throughout a lever press, segmented by four equidistant lever press duration segments (i.e. 0-25%, 25-50%, 50-75%, 75-100% of lever press duration) for significantly up-modulated and **(E)** down-modulated units in Air and CIE groups. Data points represent mean ± SEM. $^{\#}p=0.06$, * $p<0.05$, ****$p<0.0001$.

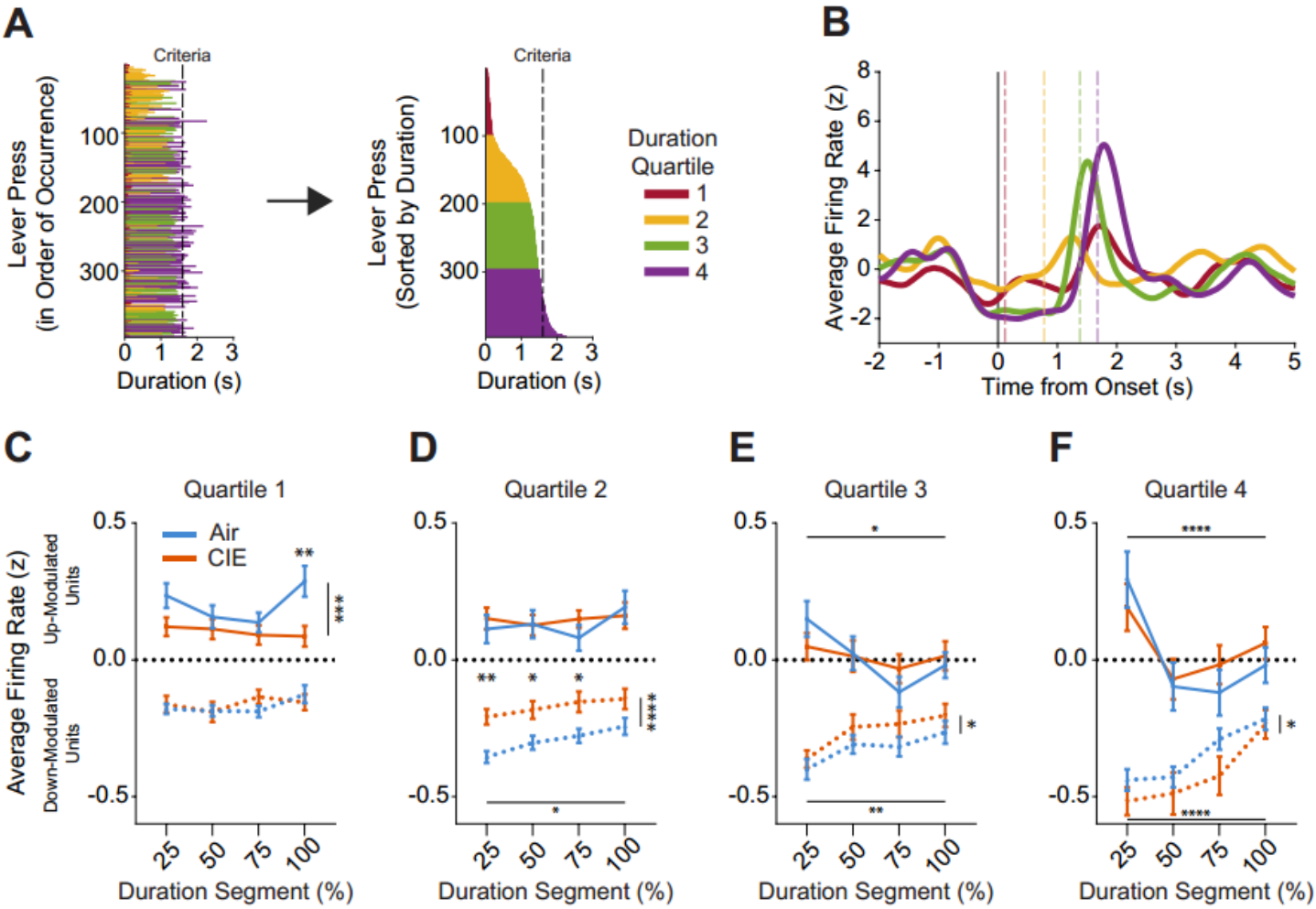

Figure 5. Dynamics of OFC activity during a lever press vary with future duration.

(A). Individual lever press events were segmented into four quartiles determined by the distribution of lever press durations within each individual recording session. **(B).** Representative unit's mean z-scored firing rates relative to the onset of a lever press. Dashed lines indicate mean lever press duration for each respective duration quartile. **(C).** Mean z-scored firing rates across duration segments of lever presses belonging to the 1st, **(D)** 2nd, **(E)** 3rd, and **(F)** 4th duration quartiles for up-modulated (top) and down-modulated units (bottom). Data points represent mean ± SEM. *p<0.05, **p< 0.01, ***p<0.001, ****p<0.0001.

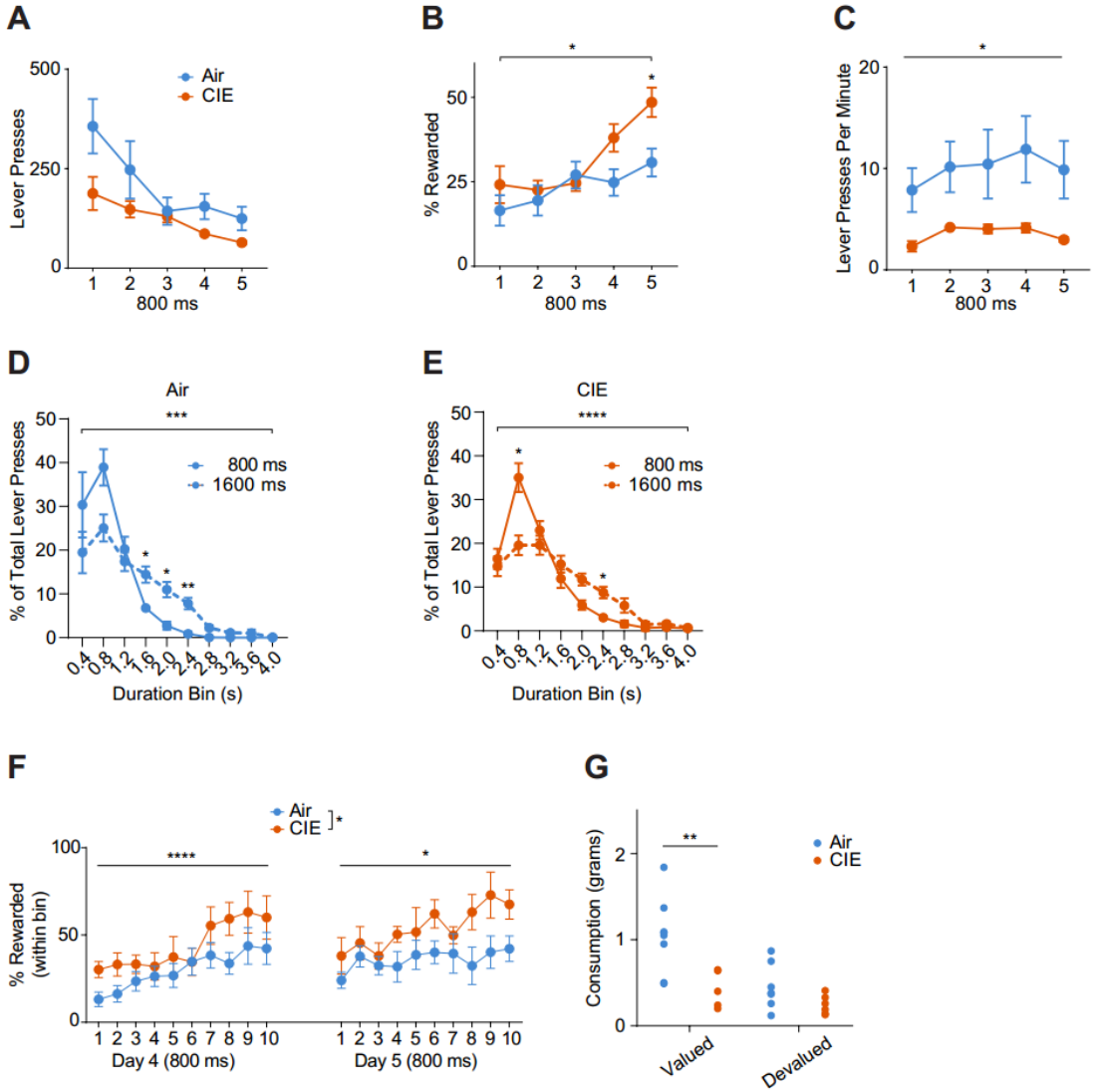

Figure 1 – figure supplement 1. Action differentiation task performance early in acquisition.

(A). Average total lever presses, **(B)** percentage of successful lever presses, and **(C)** lever pressing rate throughout 800-ms hold down duration criterion sessions. A two-way repeated measures ANOVA (Treatment x Session) on the percentage of successful lever presses found no interaction, but a main effect of Session only: $F(4, 52) = 8.72$, $p<0.0001$). A two-way repeated measures ANOVA (Treatment x Session) on the lever pressing rate found an interaction: $F(4, 52) = 4.80$, $p=0.002$; main effects of Session: $F(4, 52) = 17.34$, $p<0.0001$ and Treatment: $F(1, 13) = 5.83$, $p=0.03$. **(D).** Distribution of the percentage of total lever presses binned by duration for Air and **(E)** CIE groups. In the Air group, a two-way repeated measures ANOVA (Bin x Criteria) on the lever press duration distribution revealed an interaction: $F(9, 126) = 3.91$, $p=0.0002$, and a main effect of Bin: $F(9, 126) = 36.89$, $p<0.0001$ and Criteria: $F(1, 14) = 4.98$, $p=0.04$. In the CIE group, a two-way repeated measures ANOVA (Bin x Criteria) on the lever press duration distribution revealed an interaction: $F(9, 108) = 6.42$, $p<0.0001$, and a main effect of Bin only: $F(9, 108) = 56.71$, $p<0.0001$. **(F).** Average percentage of rewarded lever presses across normalized session duration bins during the last two days of 800-ms hold down criterion training sessions. For day 4, a Mixed-effects analysis (Bin x Treatment) found no interaction, but main effects of Bin: $F(9, 116) = 5.15$, $p <0.0001$ and Treatment: $F(1, 13) = 5.35$, $p=0.04$. For day 5, a Mixed-effects analysis (Bin x Treatment) found no interaction, but main effects of Bin: $F(9, 116) = 2.30$, $p=0.02$ and Treatment: $F(1, 13) = 6.20$, $p=0.03$. **(G).** Total grams of food pellet and 20% sucrose solution (Valued state) consumed during the 1-hour ad-libitum access feeding period before each 10-minute 1600-ms duration criterion session. Unpaired t tests with Welch's correction on total consumption revealed a difference between Air and CIE groups ($t_{10.63}=3.398$, $p=0.09$) in the Valued state, but not the Devalued state ($p>0.09$). Data points represent mean ± SEM. *$p<0.05$, **$p< 0.01$, ***$p<0.001$, ****$p<0.0001$.

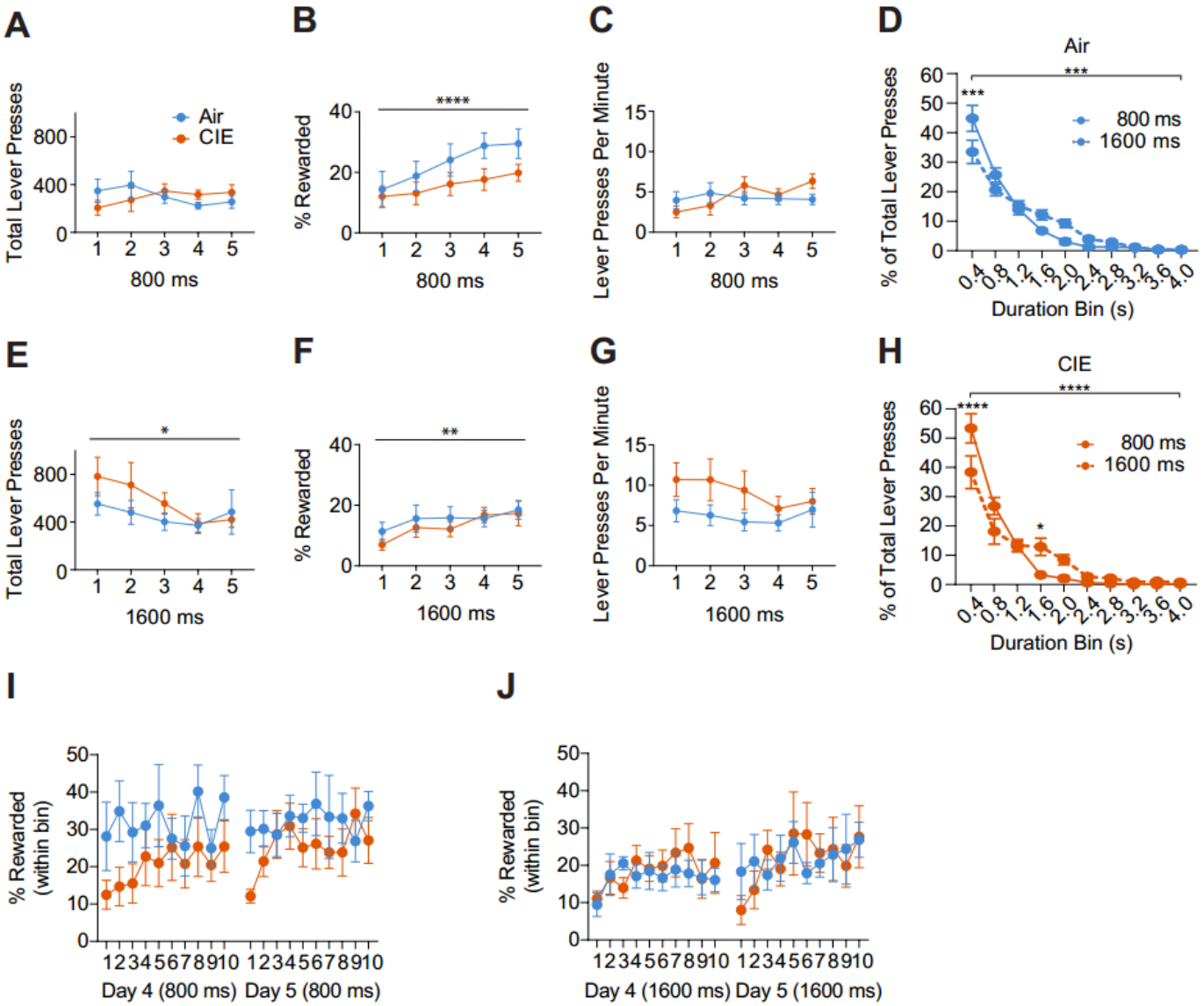

Figure 2 – figure supplement 1. Action differentiation performance in mice implanted with chronic indwelling micro-array electrodes.

(A). Average total lever presses, **(B)** percentage of successful lever presses, and **(C)** lever pressing rate throughout 800-ms hold down criteria training sessions. Mixed-effects analyses (Session x Treatment) on average total lever presses and lever pressing rate throughout 800-ms duration criterion training sessions found no interaction or main effects ($p>0.05$). A similar analysis on the percentage of successful lever presses found no interaction, but a main effect of Session only: $F(4, 62) = 7.58$, $p< <0.0001$). **(D).** Distribution of the percentage of total lever presses binned by duration for Air and **(H)** CIE groups. A two-way repeated measures ANOVA (Bin x Criteria) on the Air group's distribution revealed an interaction: $F(9, 126) = 3.67$, $p=0.0004$ and a main effect of Bin only: $F(9, 126) = 91.28$, $p<0.0001$. A similar analysis on the CIE group's distribution also revealed an interaction: $F(9, 135) = 4.29$, $p<0.0001$, and a main effect of Bin only: $F(9, 135) = 73.67$, $p<0.0001$. **(E).** Average total lever presses, **(F)** percentage of successful lever presses, and **(G)** lever pressing rate throughout 1600-ms hold down criteria training sessions. A mixed-effects analysis (Session x Treatment) on lever pressing rate throughout 1600-ms duration criterion training sessions found no interaction or main effects ($p>0.05$). Similar analyses found no interactions, but main effects of Session on the average total lever presses: $F(4, 61) = 3.005$, $p=0.03$ and the percentage of successful lever presses: $F(4, 61) = 4.369$, $p=0.004$. **(I).** Average percentage of rewarded lever presses across normalized session duration bins during the last two days of 800-ms hold down and (**J**) 1600-ms hold down criteria training sessions. Mixed-effects analyses (Session x Treatment) on each day's average percentage of rewarded lever presses found no interactions or main effects ($p>0.09$). Data points represent mean ± SEM. ***$p<0.001$, ****$p<0.0001$.

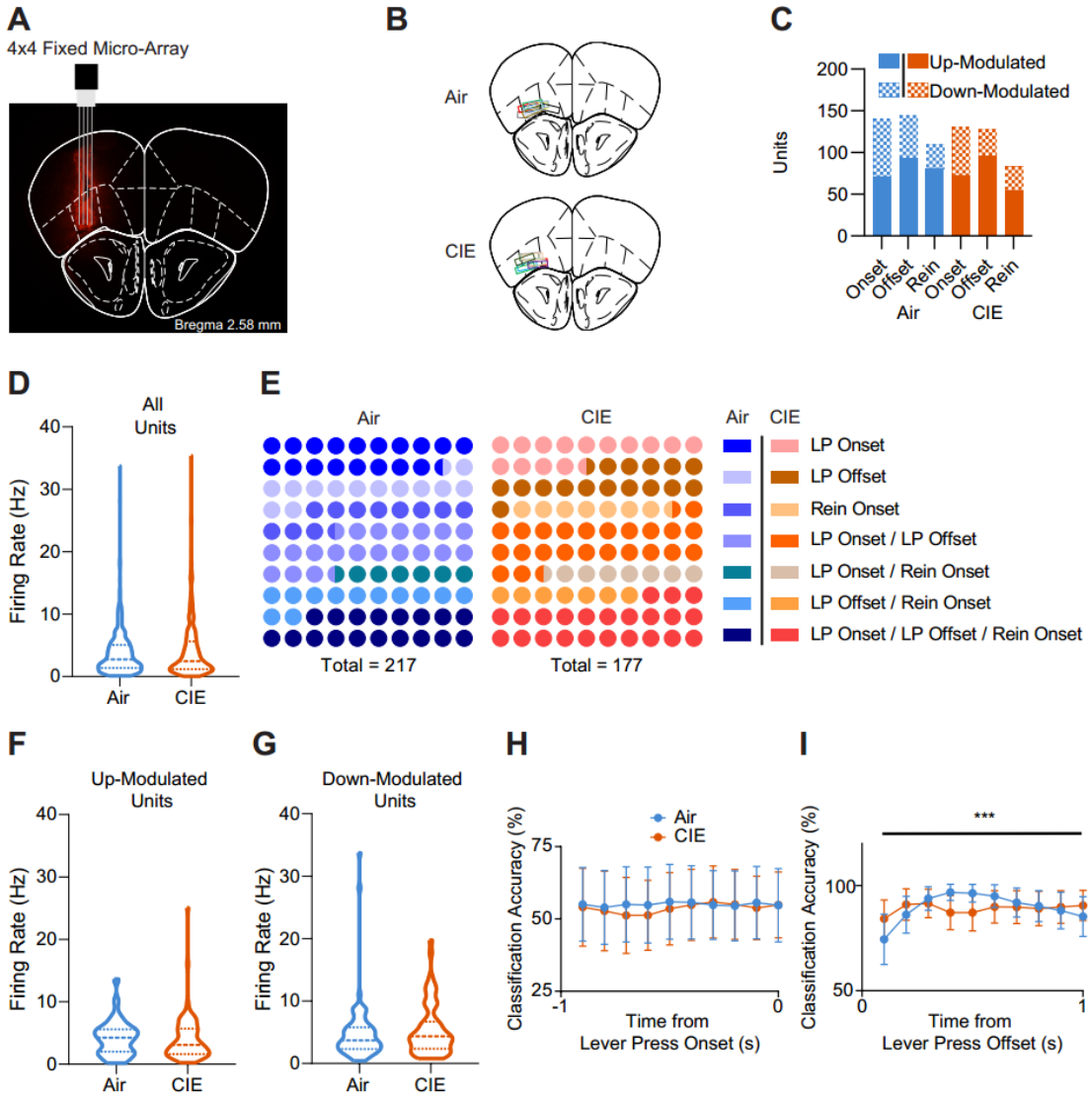

Figure 2 – figure supplement 2. Micro-array electrode placement and decoder accuracy.

(A). Representative image of fixed micro-array implant over the orbitofrontal cortex. **(B)** Implant locations segmented by Air and CIE groups. A subset of micro-arrays was dyed with a 25 mg/ml Dil (1,1′-Dioctadecyl-3,3,3′,3′-tetramethylindocarbocyanine perchlorate) solution in 200 proof ethanol for placement verification. **(C).** Total units that significantly modulated their firing rates with respect to lever press onset, offset, and food pellet reward delivery. Chi-square tests on the number of units belonging to each task component found no differences between Air and CIE groups ($p>0.12$). **(D).** Average firing rates from all captured units during a baseline period (-5 to -2 seconds before lever press onset) for Air and CIE cohorts (unpaired t test with Welch's correction: $t_{469.4}=1.333$, $p=0.18$). **(E).** Proportion of units in which spiking significantly deviated from a baseline period (-5 to -2 seconds before lever press onset) for Air and CIE cohorts. Units significantly encoded discrete task events (Lever Press Onset: Air: ~18%, CIE: ~15%; Lever Press Offset: Air: ~13%, CIE: ~16%; Reward Delivery: Air: ~11%, CIE: ~7%) as well as multiple task components (Lever Press Onset and Offset: Air: ~20%, CIE: ~24%; Lever Press Onset and Reward Delivery: Air: ~6%, CIE: ~7%; Lever Press Offset and Reward Delivery: Air: ~12%, CIE: ~7%; Lever Press Onset, Offset, and Reward Delivery: ~18%, CIE: ~23%). A chi-square test on the number of units belonging to each event type found no difference between Air and CIE groups ($p>0.24$). **(F).** Firing rates from significantly up-modulated units during a baseline period (-5 to -2 seconds before lever press onset) for Air and CIE cohorts (unpaired t test with Welch's correction: $t_{132.7}=0.2656$, $p=0.79$). **(G).** Firing rates from significantly down-modulated units during a baseline period (-5 to -2 seconds before lever press onset) for Air and CIE cohorts (unpaired t test with Welch's correction: $t_{127.0}=0.5911$, $p=0.56$). **(H).** Binned average of decoder classification accuracy over 10 cross-validation splits with respect to lever press onset and **(I)** lever press offset.

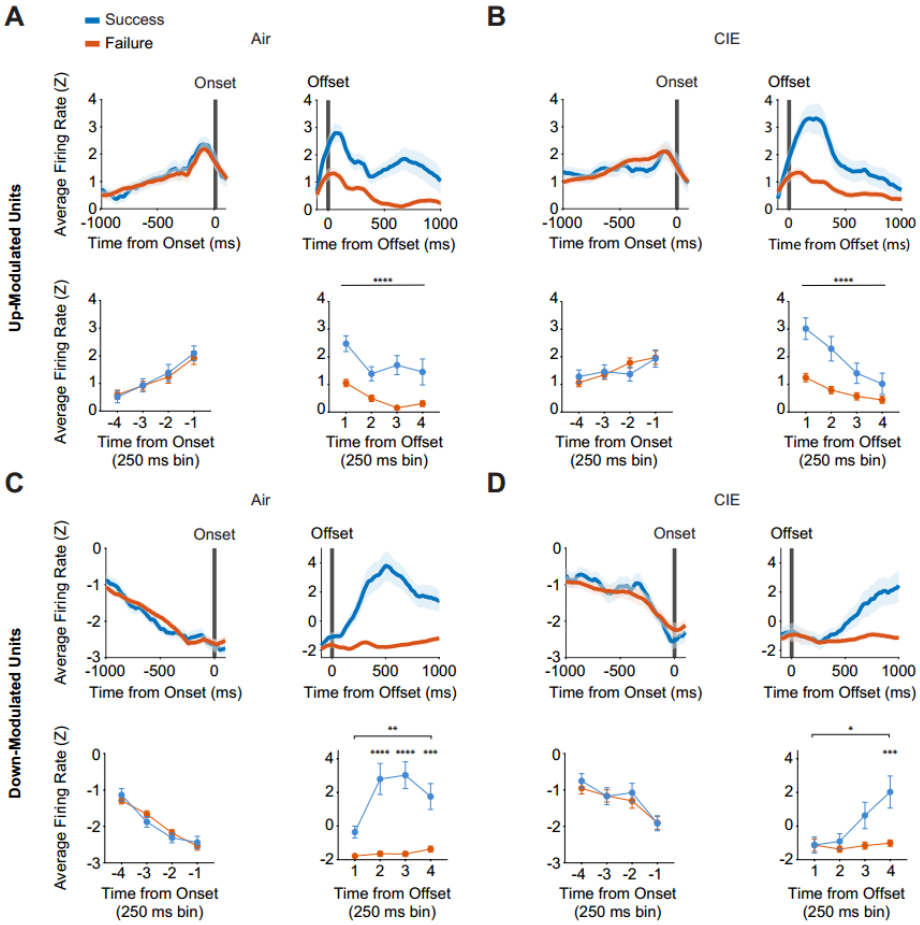

Figure 3 – figure supplement 1. OFC activity reflects lever press performance outcomes.

(A). Air and **(B)** CIE group's mean Z-scored firing rates (top) of significantly up-modulated units segmented by whether lever press successfully exceeded the 1600-ms duration criterion or not, displayed relative to lever press onset (left) or offset (right). Mean Z-scored firing rates were compared across four 250-ms bins relative to each task event (bottom). For the Air group, a two-way ANOVA (Bin x Outcome) on activity prior to lever press onset revealed no interaction, but a main effect of Bin only: $F(3, 560) = 14.47$, $p<0.0001$. A two-way ANOVA (Bin x Outcome) on activity following lever press offset revealed no interaction, but main effects of Bin: $F(3, 736) = 5.41$, $p=0.001$, and Outcome: $F(1, 736) = 46.77$, $p<0.0001$. For the CIE group, a two-way ANOVA (Bin x Outcome) on activity prior to lever press onset revealed no interaction, but a main effect of Bin only: $F(3, 568) = 4.19$, $p=0.006$. A two-way ANOVA (Bin x Outcome) on activity following lever press offset revealed no interaction, but main effects of Bin: $F(3, 760) = 8.816$, $p<0.0001$, and Outcome: $F(1, 760) = 31.08$, $p<0.0001$. **(C).** Air and **(D)** CIE group's mean Z-scored firing rates (top) of significantly down-modulated units segmented by whether lever press successfully exceeded the 1600-ms duration criterion or not, displayed relative to lever press onset (left) or offset (right). Mean Z-scored firing rates were compared across four 250-ms bins relative to each task event (bottom). For the Air group, a two-way ANOVA (Bin x Outcome) on activity prior to lever press onset revealed no interaction, but a main effect of Bin only: $F(3, 552) = 37.13$, $p<0.0001$. A two-way ANOVA (Bin x Outcome) on activity following lever press offset revealed an interaction: $F(3, 408) = 3.9$, $p=0.009$, and main effects of Bin: $F(3, 408) = 4.52$, $p=0.004$, and Outcome: $F(1, 408) = 81.83$, $p<0.0001$. Post-hoc comparisons on the Air group's down-modulated activity found differences between successes and failures in bins 2, 3, and 4 ($p<0.001$). For the CIE group, a two-way ANOVA (Bin x Outcome) on activity prior to lever press onset revealed no interaction, but a main effect of Bin only: $F(3, 464) = 9.77$, $p<0.0001$. A two-way ANOVA (Bin x Outcome) on activity following lever press offset revealed an interaction: $F(3, 248) = 3.41$, $p=0.02$, and main effects of Bin: $F(3, 248) = 4.54$, $p=0.004$, and Outcome: $F(1, 248) = 12.79$, $p=0.0004$. Post-hoc comparisons on the CIE group's down-modulated activity found differences between successes and failures in bin 4 ($p<0.001$). Data points represent mean ± SEM. *$p<0.05$, **$p< 0.01$, ***$p<0.001$, ****$p<0.0001$.

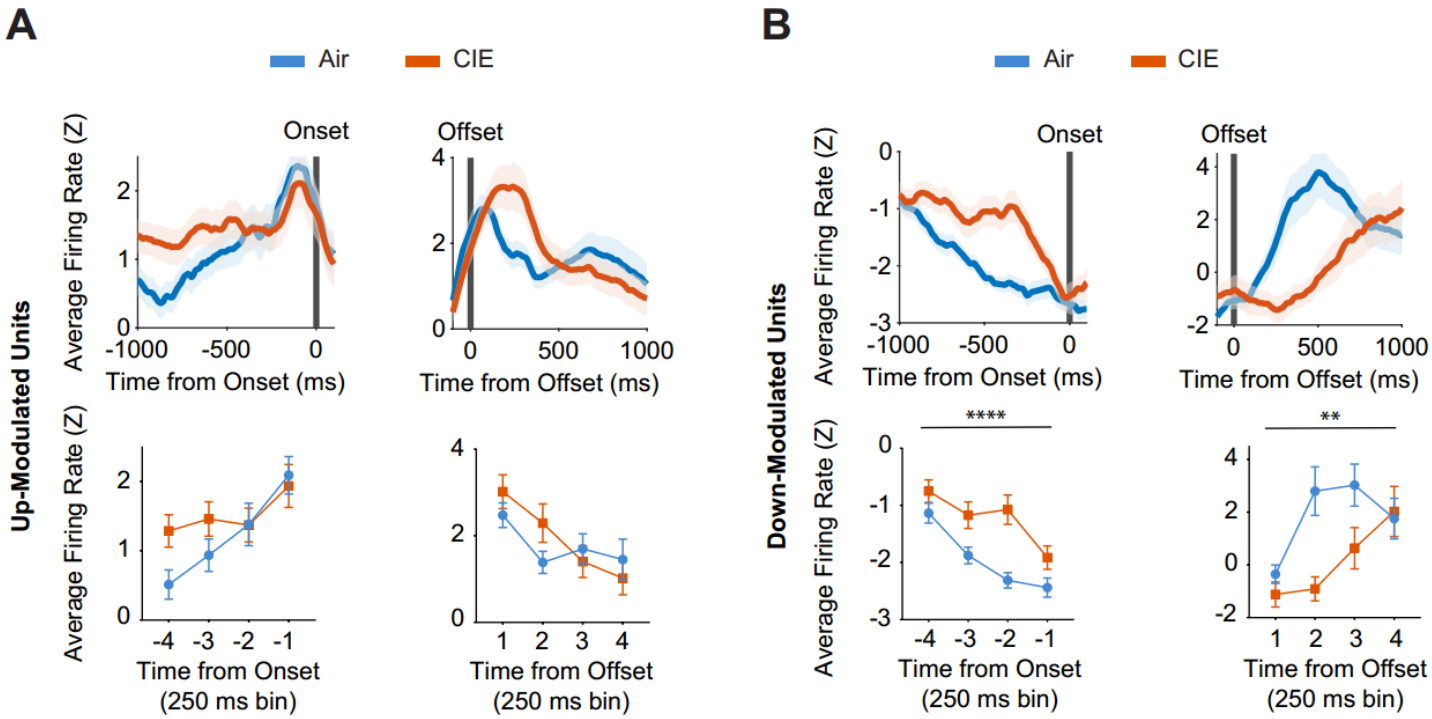

Figure 3 – figure supplement 2. Successful decisions recruit similar levels of OFC up-modulation, but not down-modulation, following chronic alcohol or air exposure.

(A). Mean Z-scored firing rates (top) comprised of lever presses that successfully exceeded the hold down criteria (1600-ms) for significantly up-modulated or (**B**) down-modulated units in Air and CIE groups before lever press onset (left) and after offset (right). Mean Z-scored firing rates were compared across four 250-ms bins relative to each task event (bottom). For down-modulated units, a two-way ANOVA (Bin x Treatment) on activity prior to lever press onset revealed no interaction, but main effects of Bin: $F(3, 508) = 14.44$, $p<0.0001$ and Treatment: $F(1, 508) = 28.36$, $p<0.0001$. A similar analysis on down-modulated activity following lever press offset revealed no interaction, but main effects of Bin: $F(3, 328) = 5.03$, $p=0.002$, and Treatment: $F(1, 328) = 9.10$, $p=0.003$. Data points represent mean ± SEM. **p< 0.01, ****p<0.0001.

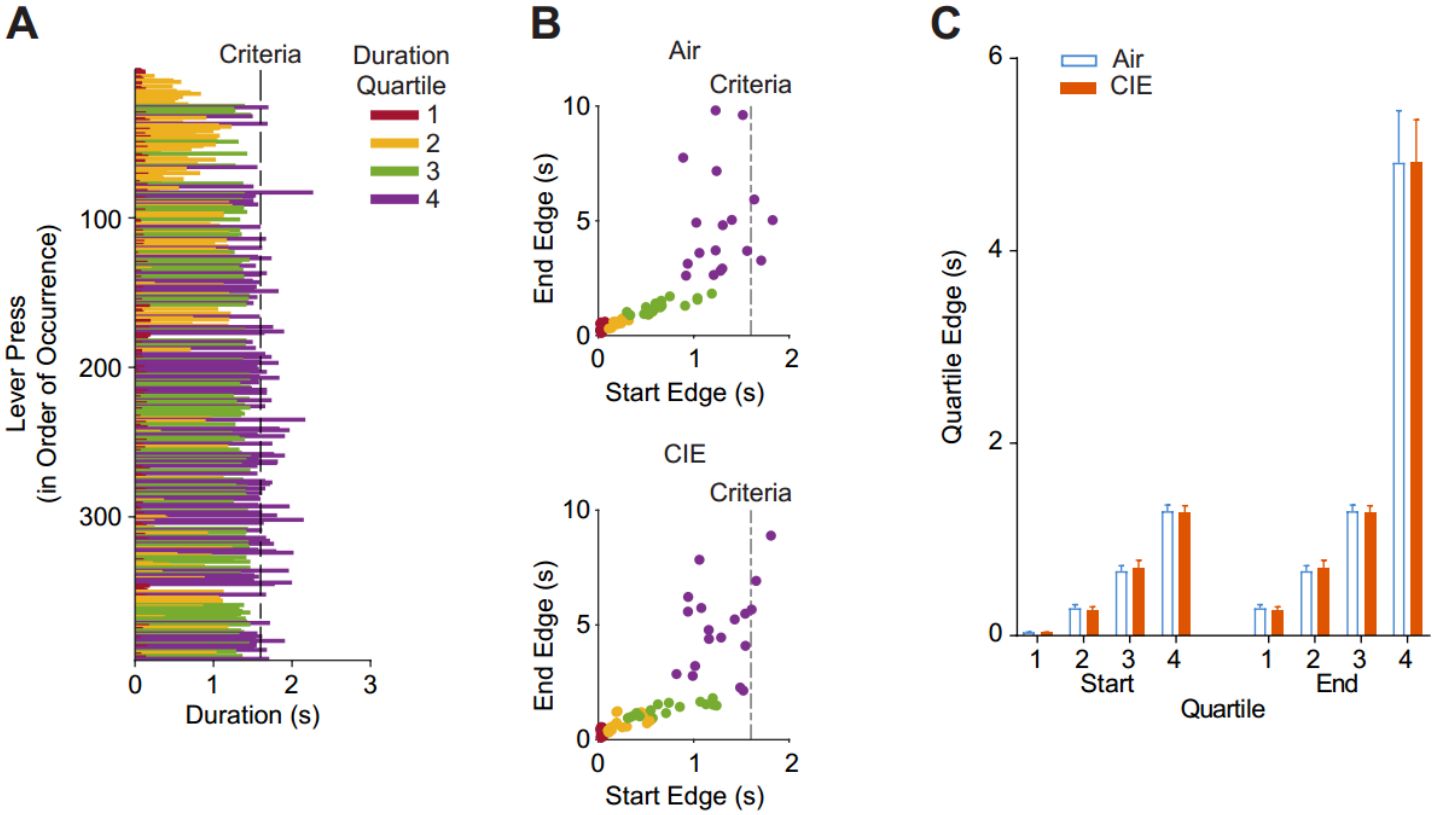

Figure 5 – figure supplement 1. Quantiles bin edges were determined by lever press duration distribution.

(A). Examples session in which lever press durations were binned into four quartiles determined by the distribution of lever press durations (left). **(B-C).** Quartile duration bin edges were similar between groups across the last two 1600-ms hold down criteria sessions that were included in our spike analyses (two-way ANOVA (Edge x Treatment), no interaction; main effect of Edge only: $F(7, 272) = 150.1$, $p<0.0001$). Data points represent mean ± SEM.

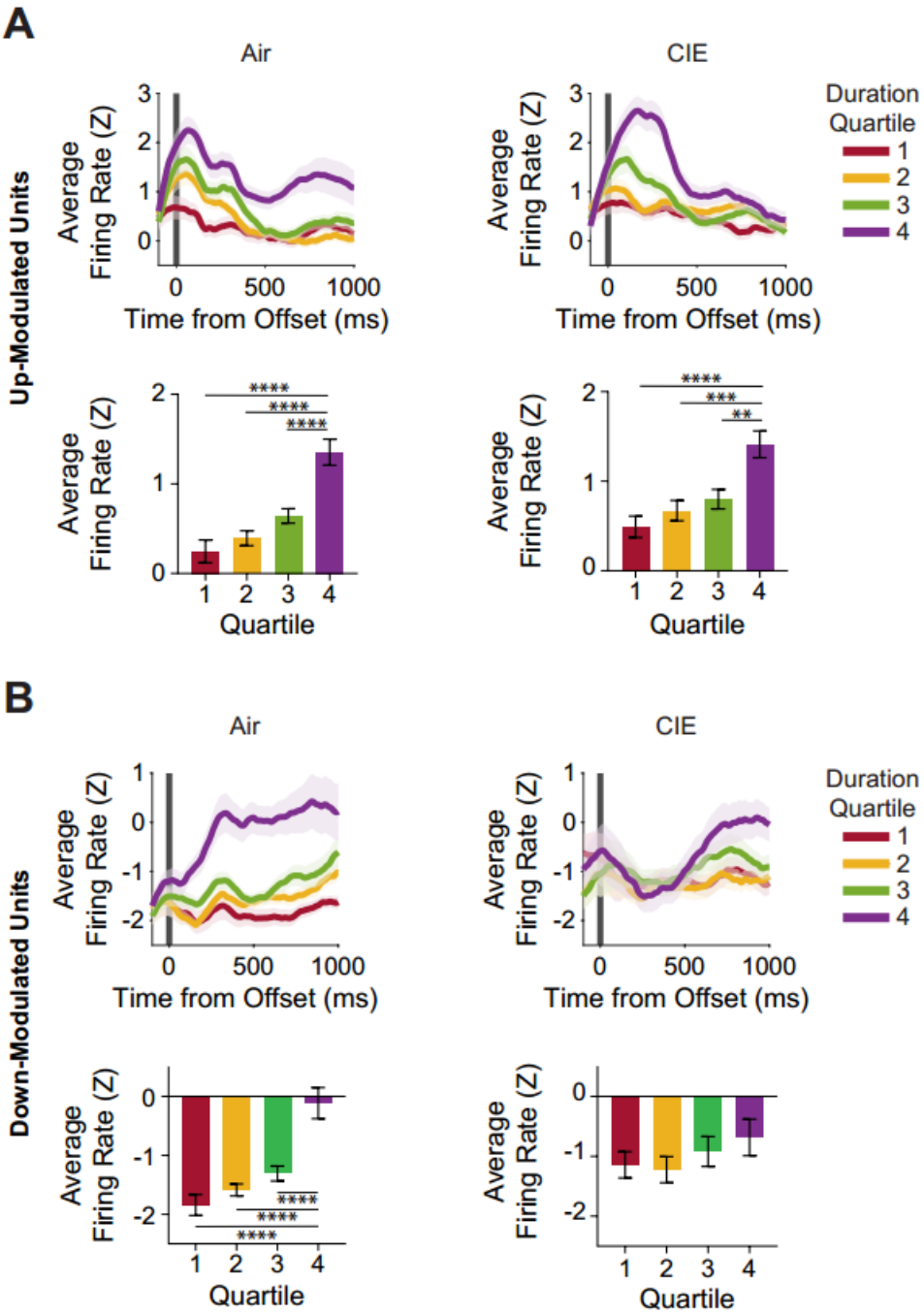

Figure 5 – figure supplement 2. OFC activity reflecting lever press durations is altered by chronic alcohol exposure.

(A). Mean Z-scored firing rates (top) comprised of all lever presses, segmented by duration quartiles, for significantly up-modulated or **(B)** down-modulated units in Air (left) and CIE (right) groups before lever press offset. Mean Z-scored firing rates were compared across quartile bins relative to offset (bottom). Ordinary one-way ANOVAs (Quartile) revealed mean activity differences ($p < 0.0001$) in Air group's up-modulated and down-modulated units. A similar analysis in CIE group's unit activity revealed differences ($p < 0.0001$) in up-modulated units only. No differences were found in the firing rates between quartiles in CIE down-modulated units ($p=0.43$). Data points represent mean ± SEM. **p< 0.01, ***p<0.001, ****p<0.0001.

Figure 1 - Figure Supplement 1

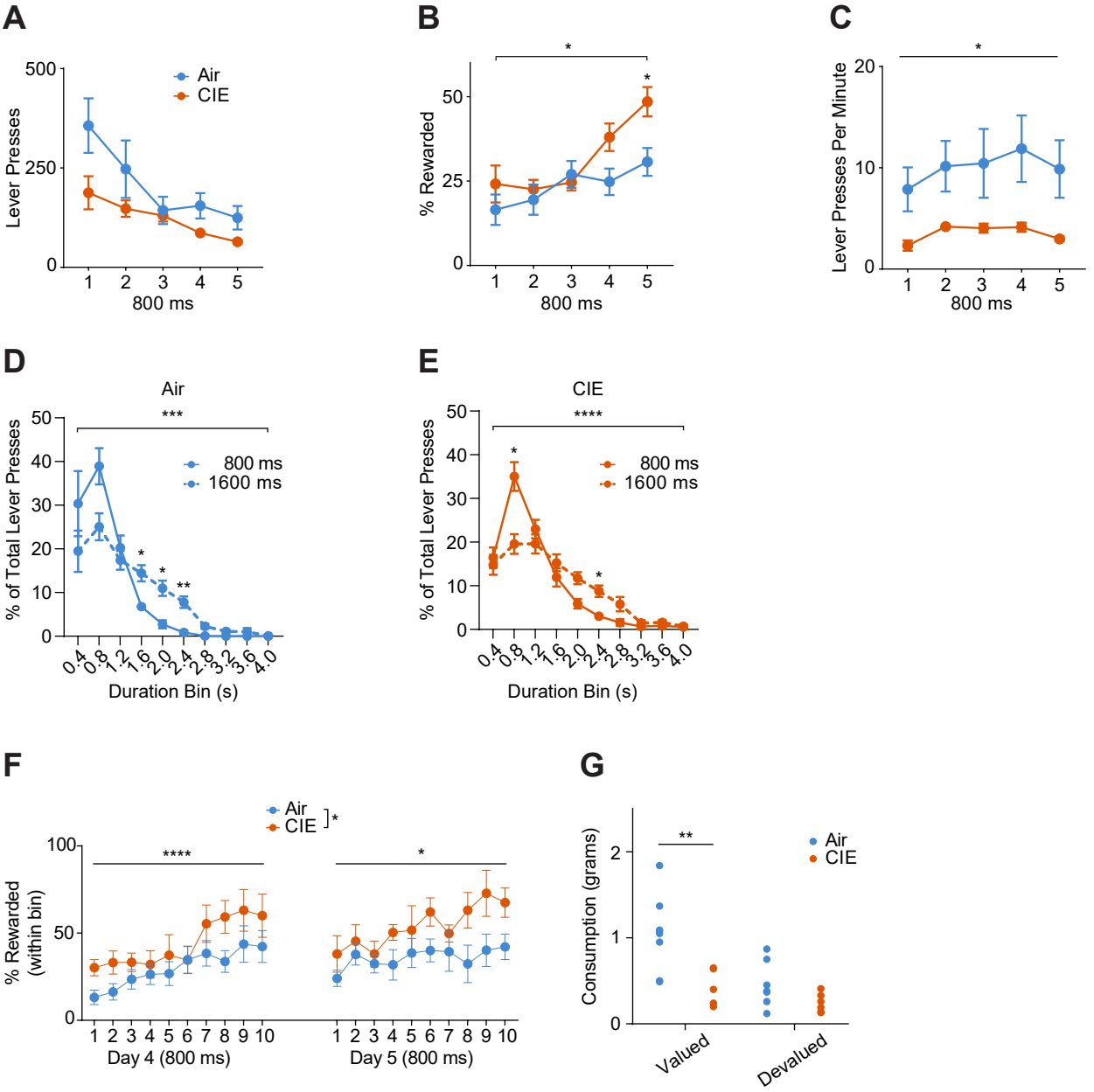

Figure 1

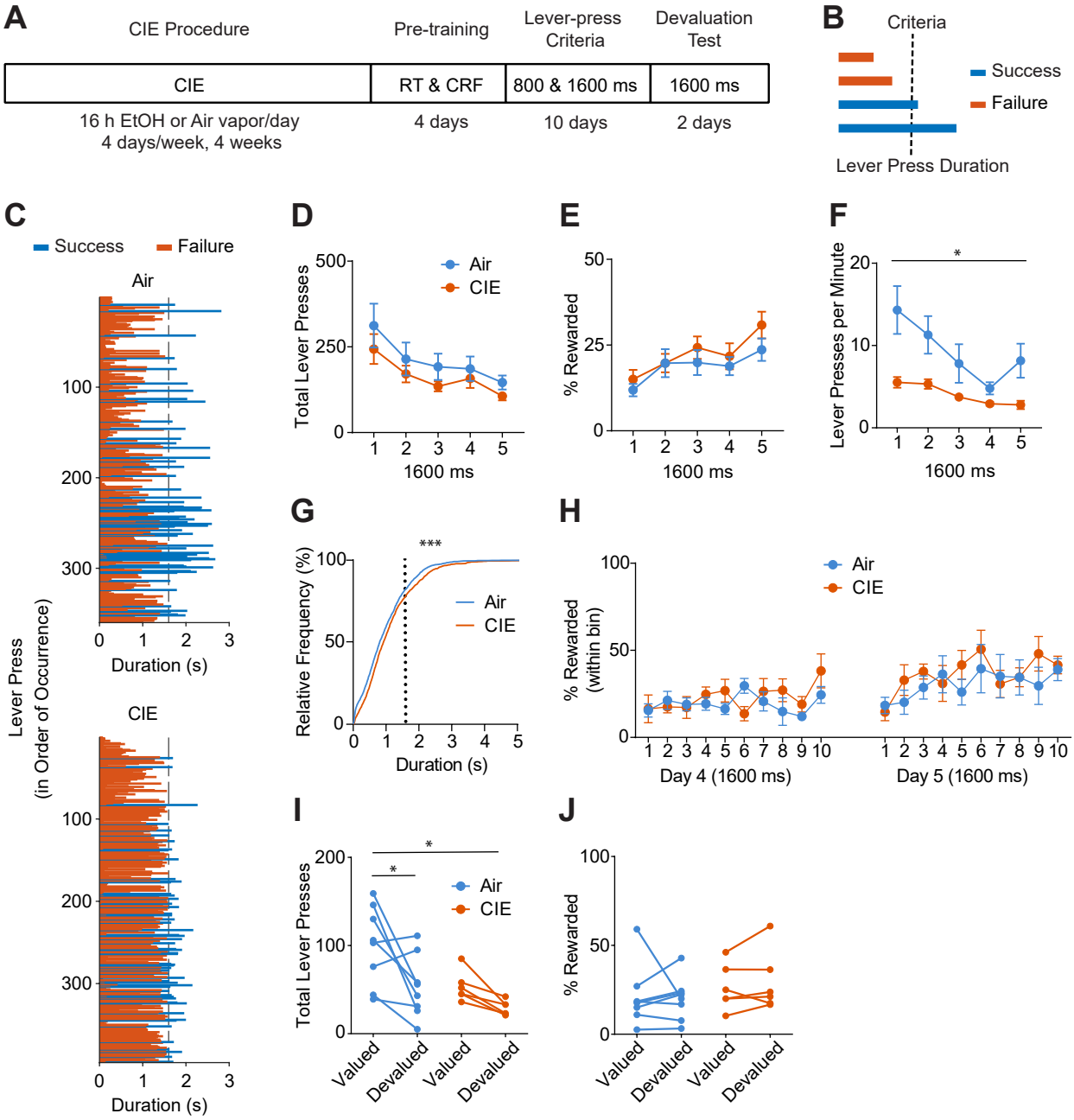
A
CIE Procedure
Pre-training
Lever-press Criteria
Devaluation Test
CIE
RT & CRF
800 & 1600 ms
1600 ms
16 h EtOH or Air vapor/day
4 days/week, 4 weeks
4 days
10 days
2 days
B
Criteria
Success
Failure
Lever Press Duration
C
Success
Failure
Air
CIE
Lever Press
(in Order of Occurrence)
Duration (s)
D
Total Lever Presses
Air
CIE
1600 ms
E
% Rewarded
1600 ms
F
Lever Presses per Minute
1600 ms
G
Relative Frequency (%)
Duration (s)
H
% Rewarded
(within bin)
Day 4 (1600 ms)
Day 5 (1600 ms)
I
Total Lever Presses
Valued
Devalued
J
% Rewarded

Figure 2 - Figure Supplement 1

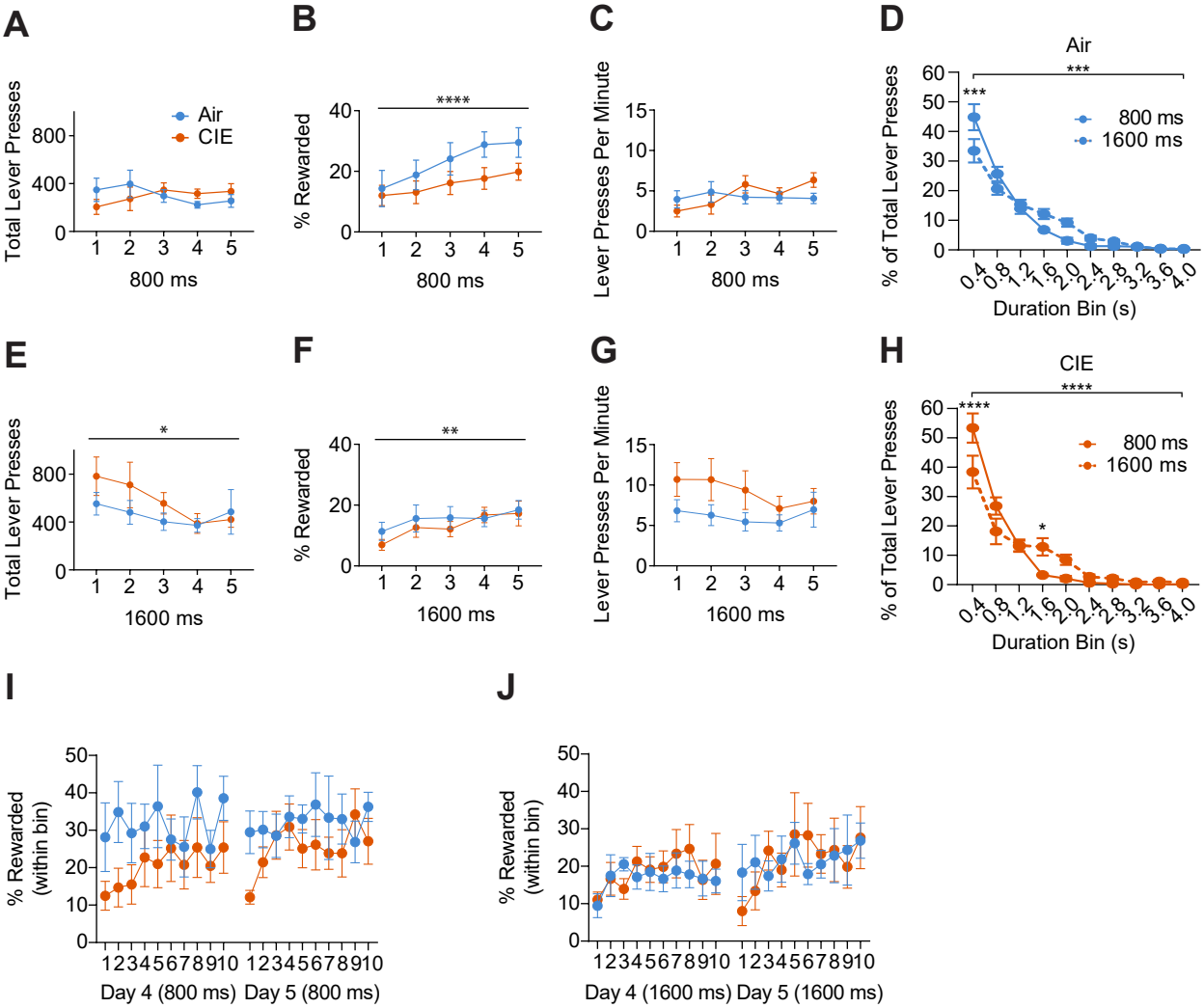

Figure 2 - Figure Supplement 2

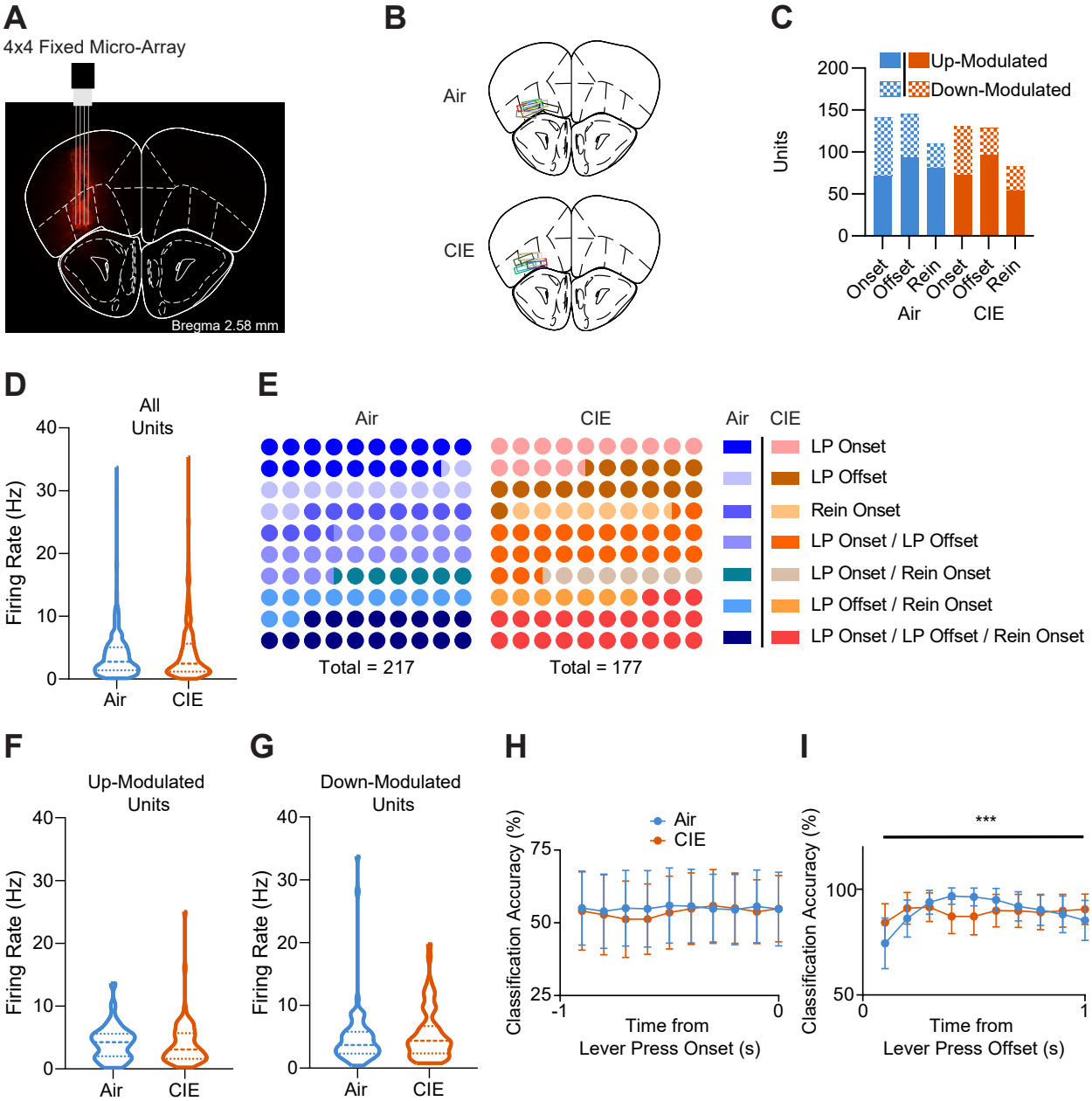

Figure 2

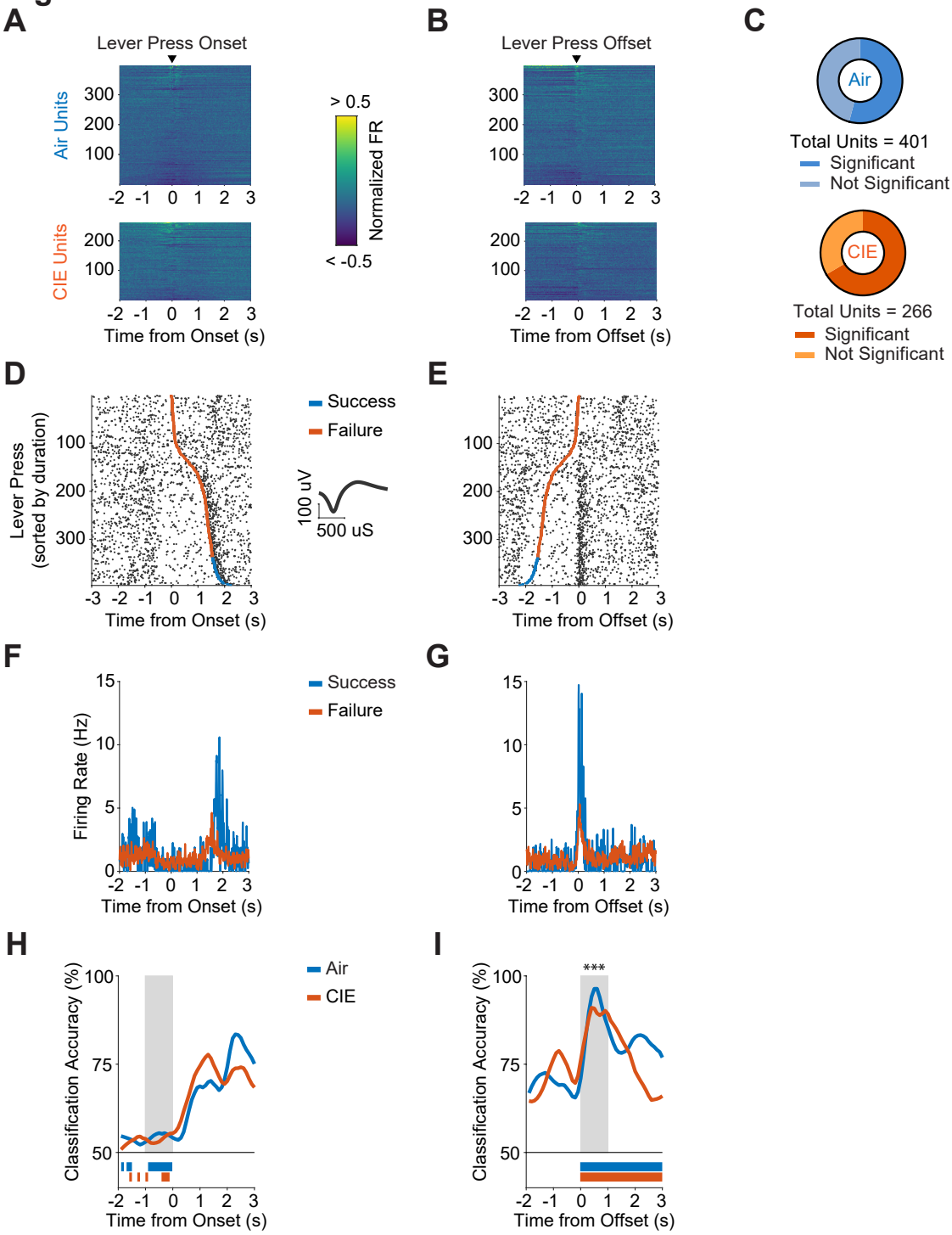
A
Lever Press Onset
Air Units
300
200
100
CIE Units
200
100
-2 -1 0 1 2 3
Time from Onset (s)
> 0.5
Normalized FR
< -0.5
B
Lever Press Offset
300
200
100
200
100
-2 -1 0 1 2 3
Time from Offset (s)
C
Air
Total Units = 401
Significant
Not Significant
CIE
Total Units = 266
Significant
Not Significant
D
Lever Press
(sorted by duration)
100
200
300
-3 -2 -1 0 1 2 3
Time from Onset (s)
Success
Failure
100 uV
500 uS
E
100
200
300
-3 -2 -1 0 1 2 3
Time from Offset (s)
F
Firing Rate (Hz)
15
10
5
0
-2 -1 0 1 2 3
Time from Onset (s)
Success
Failure
G
15
10
5
0
-2 -1 0 1 2 3
Time from Offset (s)
H
Classification Accuracy (%)
100
75
50
-2 -1 0 1 2 3
Time from Onset (s)
Air
CIE
I
Classification Accuracy (%)
***
100
75
50
-2 -1 0 1 2 3
Time from Offset (s)

Figure 3 - Figure Supplement 1

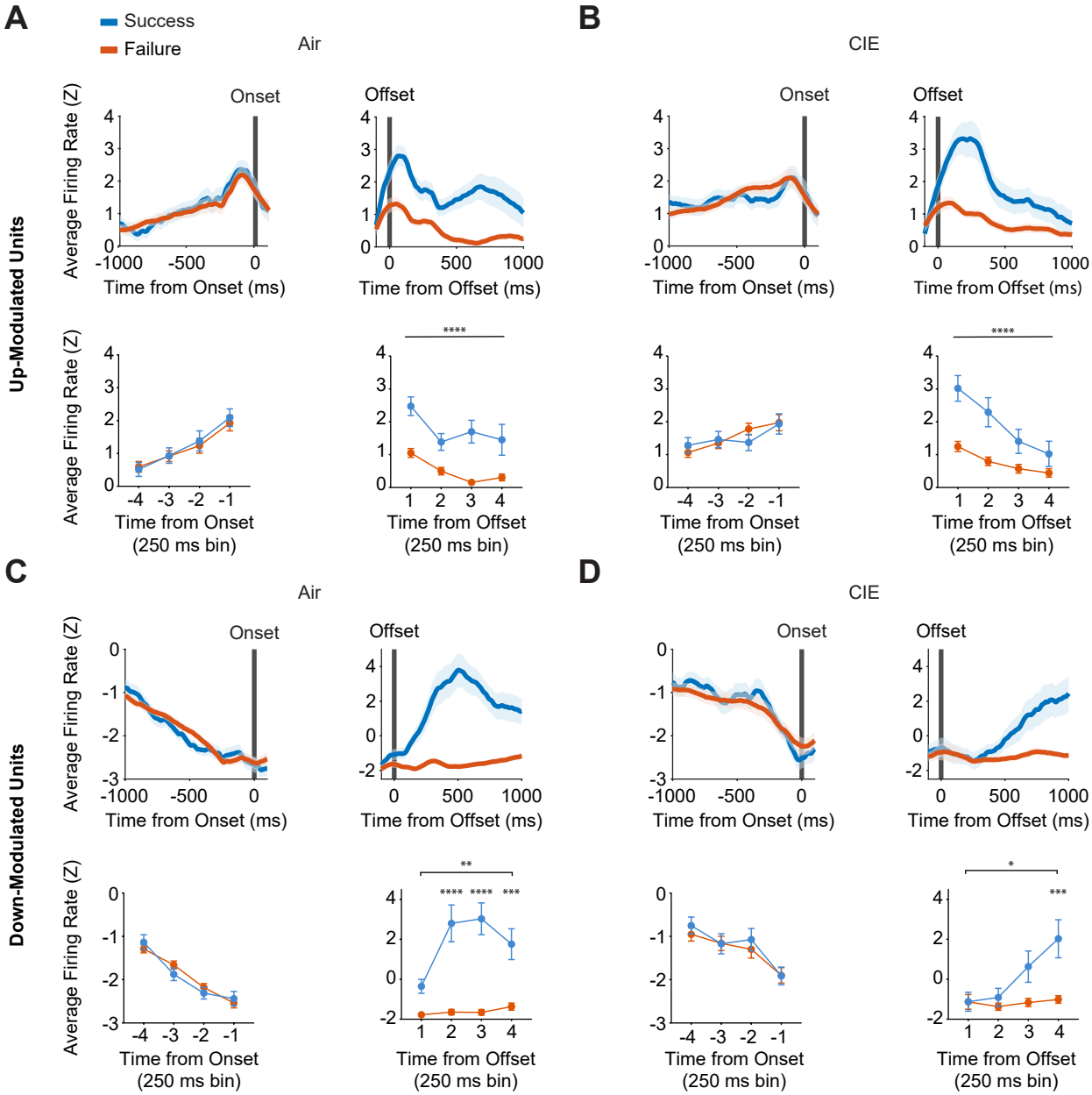

Figure 3 - Figure Supplement 2

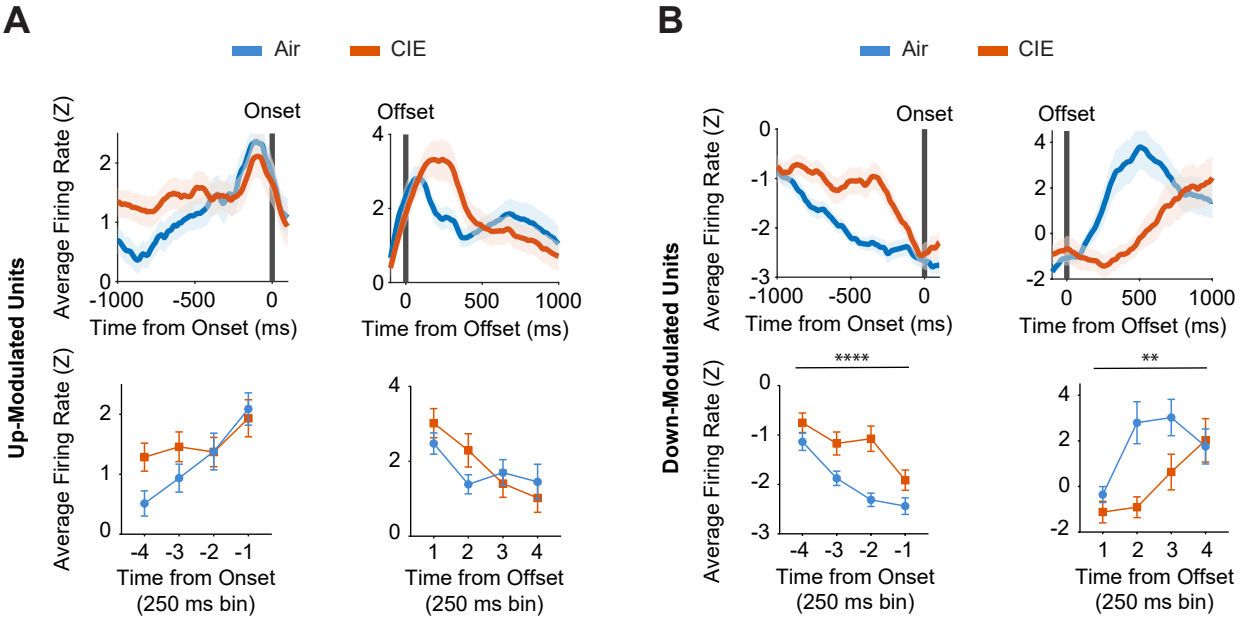

Figure 3

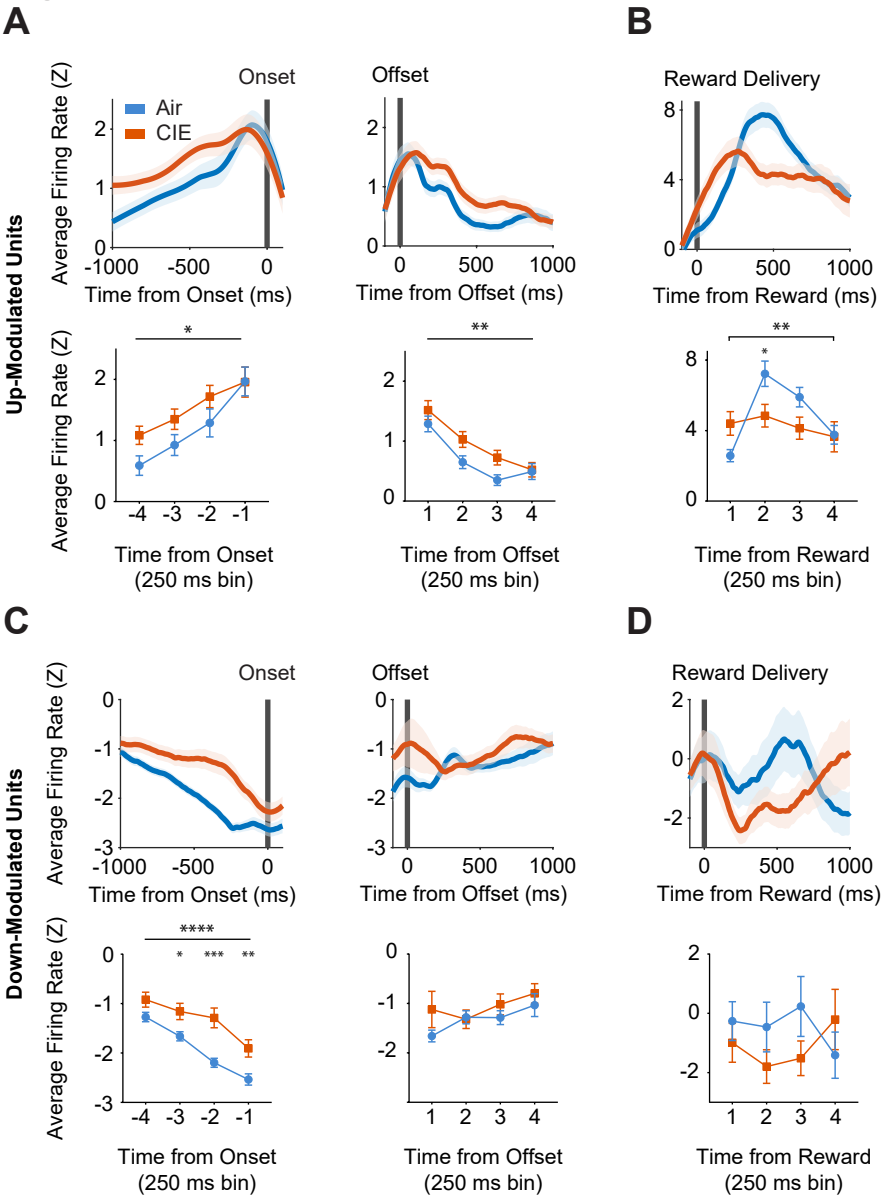
A
B
C
D
Up-Modulated Units
Down-Modulated Units
Onset
Offset
Reward Delivery
Air
CIE
Average Firing Rate (Z)
Time from Onset (ms)
Time from Offset (ms)
Time from Reward (ms)
Time from Onset (250 ms bin)
Time from Offset (250 ms bin)
Time from Reward (250 ms bin)
*
**
****
***

Figure 4

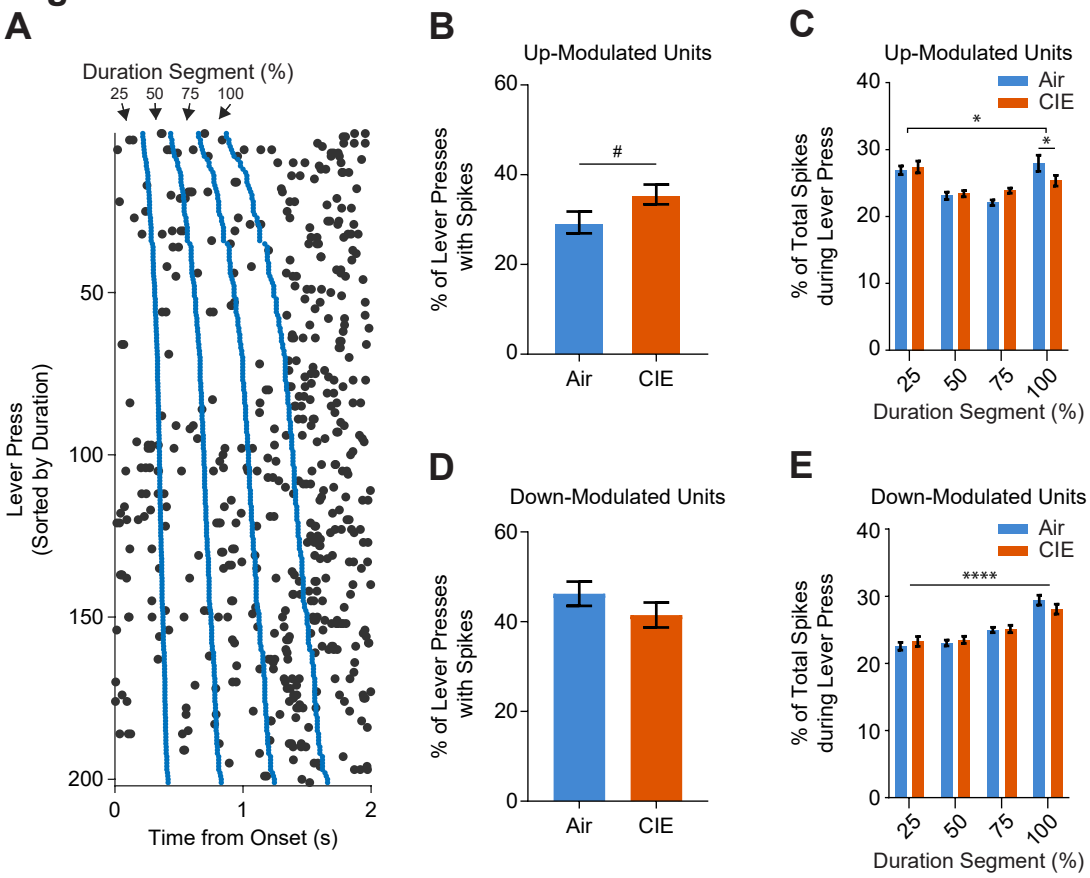
A
Duration Segment (%)
25
50
75
100
Lever Press
(Sorted by Duration)
50
100
150
200
0
1
2
Time from Onset (s)
B
Up-Modulated Units
% of Lever Presses
with Spikes
60
40
20
0
#
Air
CIE
C
Up-Modulated Units
Air
CIE
% of Total Spikes
during Lever Press
40
30
20
10
0
*
*
25
50
75
100
Duration Segment (%)
D
Down-Modulated Units
% of Lever Presses
with Spikes
60
40
20
0
Air
CIE
E
Down-Modulated Units
Air
CIE
% of Total Spikes
during Lever Press
40
30
20
10
0
****
25
50
75
100
Duration Segment (%)

Figure 5 - Figure Supplement 1

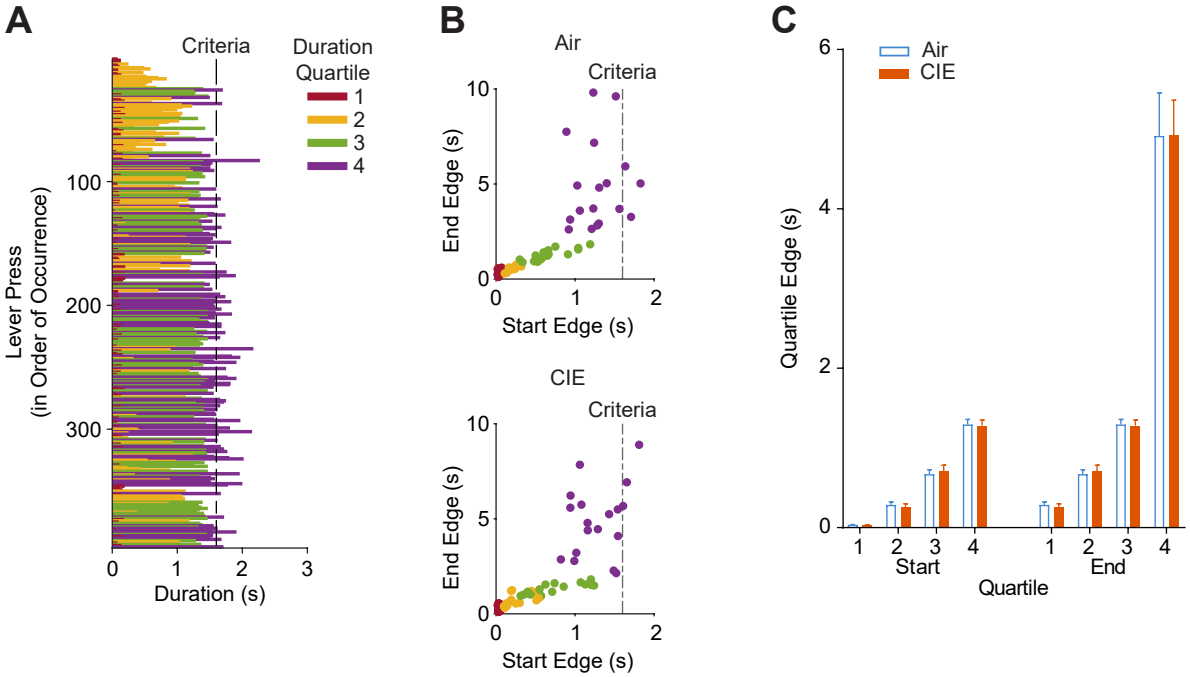

Figure 5 - Figure Supplement 2

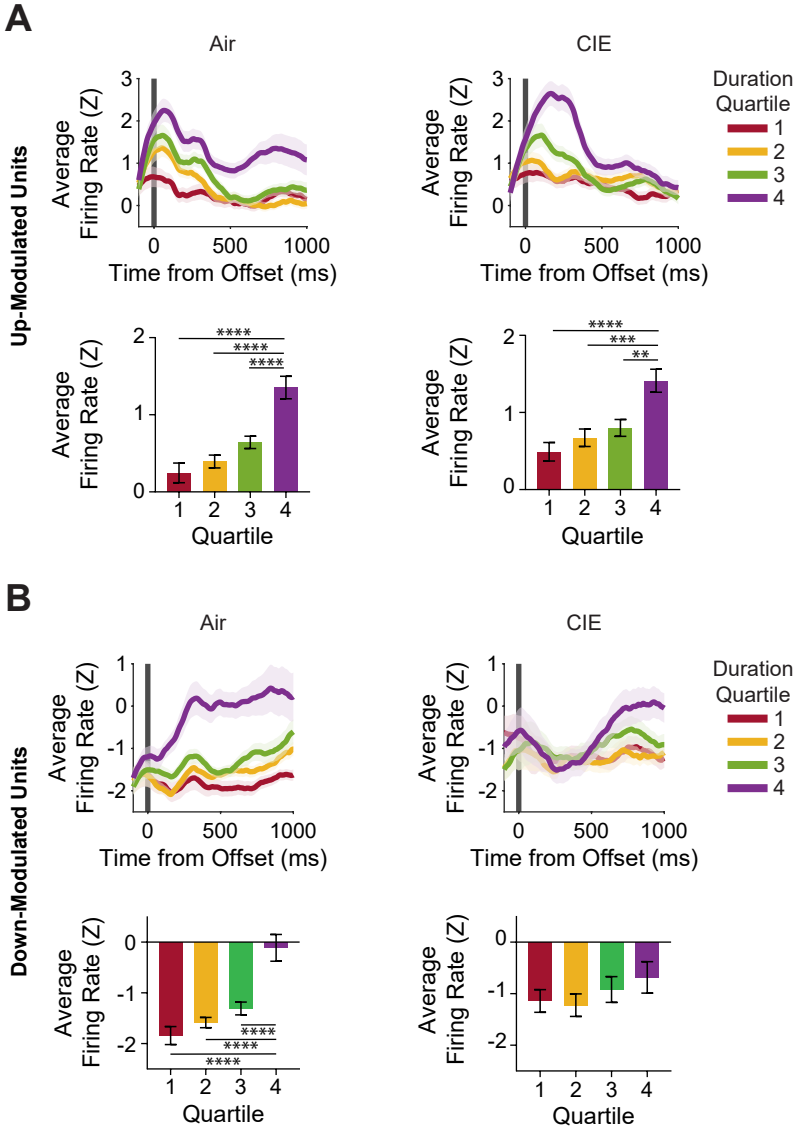

Figure 5

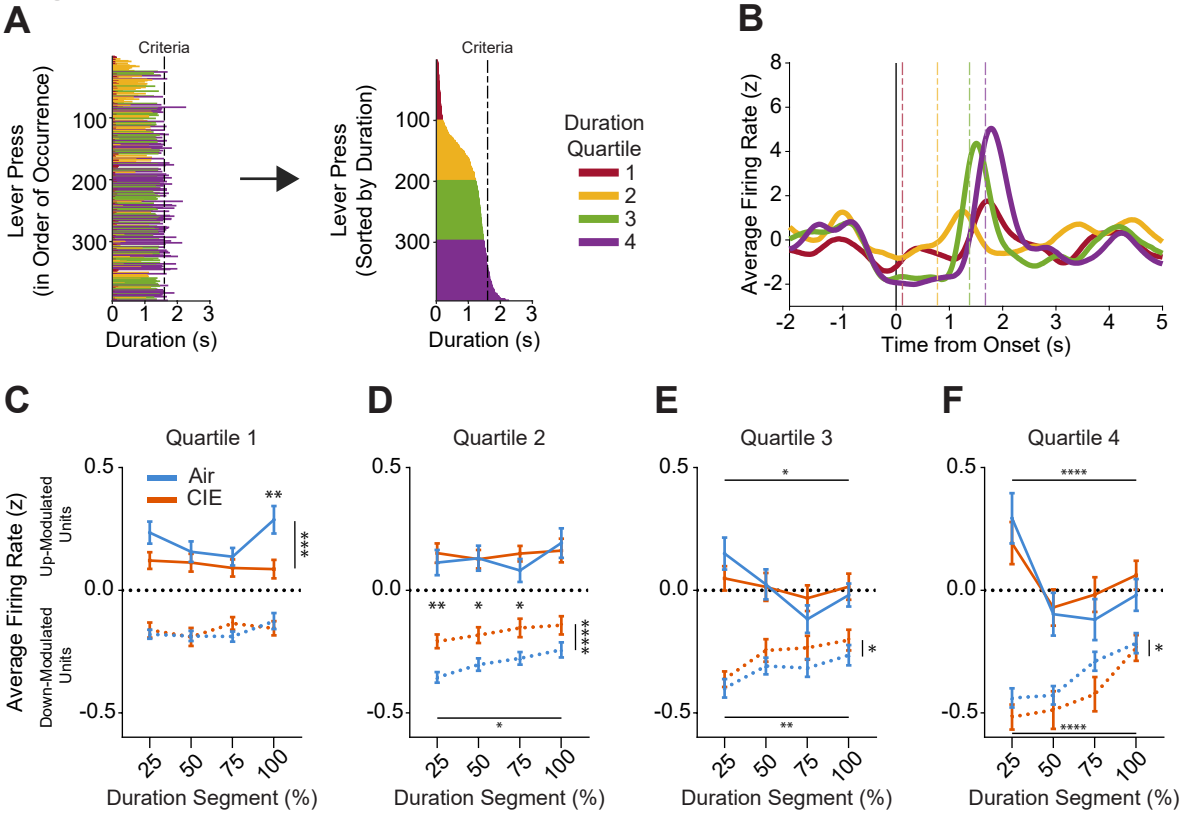
A
Criteria
Lever Press
(in Order of Occurrence)
100
200
300
0 1 2 3
Duration (s)
Criteria
Lever Press
(Sorted by Duration)
Duration
Quartile
1
2
3
4
B
Average Firing Rate (z)
Time from Onset (s)
C
Quartile 1
Air
CIE
Up-Modulated Units
Down-Modulated Units
Average Firing Rate (z)
Duration Segment (%)
D
Quartile 2
E
Quartile 3
F
Quartile 4